Chapter 9

Partition coefficients, volumes of distribution, and tissue composition

9-1. Introduction: Tissue/blood partition coefficients and influencing factors
9-2. The partition coefficient, l, and electrochemical equilibria
    9-2.1. Oil/water partitioning
    9-2.2. Tissue/blood partitioning
    9-2.3. Partitioning in tissue
    9-2.4. Passive equilibration
    9-2.5. Molecular exclusion
    9-2.6. The effects of charge
    9-2.7. Intraregional binding enlarges the partition coefficient
    9-2.8. Transmembrane electrochemical potentials influence λ
    9-2.9. pH affects partitioning of acids and bases
9-3. Anatomic and virtual volumes
9-4. Volume and specific gravity of tissue components
    9-4.1. An experimental procedure for intraorgan volumes of distribution
    9-4.2. Definition
    9-4.3. Applying conservation principles to masses and volumes
    9-4.4. From composition back to partition coefficients
9-5. Kinetics of dilution and distribution
9-6. Dilution in a well-stirred volume
    9-6.1. Fluid displacement from a well-stirred tank or perfect mixing chamber
    9-6.2. Impeded mixing
9-7. Two regions with flow mixing
9-8. Plasma space estimation when tracer is lost
9-9. Summary
9-10. Problems
9-11. Further reading
9-12. References

9-1. Introduction: Tissue/blood partition coefficients and influencing factors

In order to interpret observations of the kinetics of tracer solute transport within an organ, we need to understand the mechanisms and routes of exchange that affect the tracer and its steady-state (equilibrium) behavior. The solute's tissue-to-plasma partition coefficient, which is the steady-state ratio of a tracer solute's region-to-plasma concentration, and the related measure, the tracer solute's volume of distribution, are both used in the interpretation of rates of exchange or washout.

We start with a straightforward concept—that the volume of a tissue can be calculated from the amount of a solute in that tissue divided by the average concentration:

$$V = q_0 / C . \tag{9-1}$$

Experimentally, one would usually work the other way, by calculating the concentration from the amount of solute divided by the volume, but here we wish to see how to extend the expression to situations where the volume is not directly measurable. Later, we introduce "virtual volumes of distribution", which are factors in determining the rate constants for exchange. For this we need prior estimates of partition coefficients and knowledge of the mechanisms that distribute solutes in tissues.

The partitioning of a solute between blood and tissue depends on the characteristics of the molecule and of the tissue. The following is a checklist of pertinent features which can be used to predict or explain the values of the blood/tissue partition coefficients, and the volumes of distribution for the solute.

1. Molecular characteristics
   - Size, hydrated, and unhydrated
   - Hydrophobicity/hydrophilicity
   - Charge and charge density
   - Shape and flexibility
2. Tissue characteristics

   Composition
   - Physical sizes of spaces for blood, ISF, cells
   - Nature of extracellular matrix

   Functions of the cells, indicating their general characteristics
   - Types of transporters
   - Lipid versus nonlipid
   - Metabolic rates
   - Membrane potential
   - pH

   Partition coefficients
   - Relative solubilities in plasma, blood, and tissues
   - Binding sites in blood, interstitium and cells
   - Specific and nonspecific binding
   - Symmetry/asymmetry of transport

The partition coefficient and volumes of distribution are measures defined for the steady state. They are not constants, but rather are influenced by physiological and biochemical conditions, and are not influenced by the kinetics of solute dilution and distribution. The rapidity with which a steady state is reached depends on physiological factors such as the blood flow to the organs of the body, the rates of permeation of vascular endothelium in various organs, the cellular exchange rates, and the heterogeneities of extravascular extracellular matrix and of circulatory system dynamics.

9-2. The partition coefficient, λ, and electrochemical equilibria

9-2.1. Oil/water partitioning

When olive oil and water are shaken vigorously together in a jar, a tracer-labeled solute, *x*, will dissolve in each of the two immiscible fluids. The final concentration in the two layers at

equilibrium is in proportion to the solubility of the solute in the two fluids (Fig. 9-1). After the solvents have separated, oil above and water below, samples are taken from each layer. The oil-to-water partition coefficient is determined from the ratio of activities or concentrations:

$$\lambda_{\text{oil/water}}(x) = \frac{\text{cpm/ml in oil}}{\text{cpm/ml in water}}. \tag{9-2}$$

Although olive oil-to-water partitioning is a traditional test for biological solutes, Stein (1986) observed that the heptane/water partition coefficient is a better index of the permeability of membranes to solutes. One reason is that olive oil, although mainly palmitic acid, is not pure and therefore some water dissolves in the olive oil. Solubility in heptane is an excellent measure of the solubility of a substance in cell membranes.

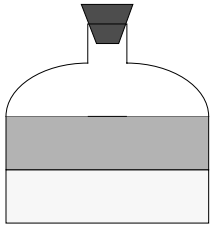

$$\lambda_{\text{oil/water}} = \frac{x_{\text{oil}}}{x_{\text{water}}}$$

Figure 9-1: A solute's oil-to-water partition coefficient is determined experimentally.

9-2.2. Tissue/blood partitioning

At tissue/blood equilibrium the concentration in the tissue may be higher or lower than in the plasma. One usually uses plasma as the reference fluid rather than whole blood, since we would not like the parameters of the system to change when the hematocrit changes. The partition coefficient for a specific solute region, *r*, is defined by its equilibrium concentration relative to that in plasma, C_{pl}:

$$\lambda_{\text{r/pl}}(\text{solute}) = C_{\text{r}} / C_{\text{pl}}. \tag{9-3}$$

We can define a partition coefficient for a solute in a tissue that contains no plasma as long as it equilibrates with plasma. An example is the partition coefficient for tissue cells that exchange with plasma via ISF. For ethanol in red cells suspended in plasma, we calculate $\lambda_{\text{RBC/pl}} = C_{\text{RBC}}/C_{\text{pl}}$. In this expression it is clear that the partition coefficient represents the ratio of solubilities in the two phases. It is in every way analogous to an oil-to-water partition coefficient, and is therefore a solubility ratio.

9-2.3. Partitioning in tissue

The situation is not quite so tidy if one takes a tissue sample and determines a concentration in it as a ratio to that in plasma, because tissue will normally contain plasma. It is correct to say that λ is the ratio of solubilities in the tissue to that in plasma, but it is not possible to define thereby the solubility in the non-plasma fraction of the tissue unless one also knows the plasma content of that tissue. So this solubility ratio loses its nice physicochemical meaning as a solubility or relative solubility.

For practical purposes we need to define "tissue". Although in casual terms we think that tissue is "not blood", it is not possible to sample tissue without some blood being trapped in the sample. Thus, in this chapter, we use "tissue" to mean "tissue with blood in the microvessels but not in the larger main arteries and veins", much as stated in Chapter 4.

These factors affect tissue/blood partitioning and volumes of distribution:

1. Tissue regional composition
   A. Fractions of water, fat, protein, solutes
   B. Water spaces in RBC, plasma, ISF and cells of varied types
   C. Steric hindrance and molecular exclusion
2. The solute's ability to traverse membranes
   A. High solubility in membrane
   B. Small molecular size
   C. Existence of specific transporter, and competitors
3. Binding sites in each region
   A. Concentrations of binding sites
   B. Affinities
   C. Association/dissociation rates
   D. Mobile versus immobile binding sites
4. For charged solutes
   A. Transmembrane potential
   B. Ionic pumps
   C. Mobile and immobile binding sites
   D. Charges on macromolecules and membrane
5. For acids and bases
   A. pH, extracellular versus intracellular
   B. pK_a
   C. Association/dissociation rates (e.g., CO_2)
6. Solute metabolism
   A. Intracellular degradation
   B. Intracellular synthesis
   C. Microcompartmentalization

The idea that a high lipid solubility leads to a high partition coefficient and a high volume of distribution is *wrong*. Lipid solubility does permit easy passage across cell membranes and does therefore give access to the lipid inside cells and to the membranes of intracellular organelles. However, the total amount of lipid, including membranes, in nonfatty tissue is low; the heart is about 2% fat (Dible, 1934). So a high heptane/water partition coefficient really means that the water solubility for the solute is low. An exemplary case is that of DMSO, which has a $\lambda_{heptane/water}$ of about 200. Figure 9-2 shows the outflow dilution curves from an isolated perfused rabbit heart for DMSO and two reference substances, intravascular albumin and THO. The DMSO curve is only modestly delayed compared to albumin despite the fact that the membrane's permeability to DMSO is essentially infinite, and because of the low solubility in water the volume of distribution is only about twice that of the plasma space, and less than the water space..

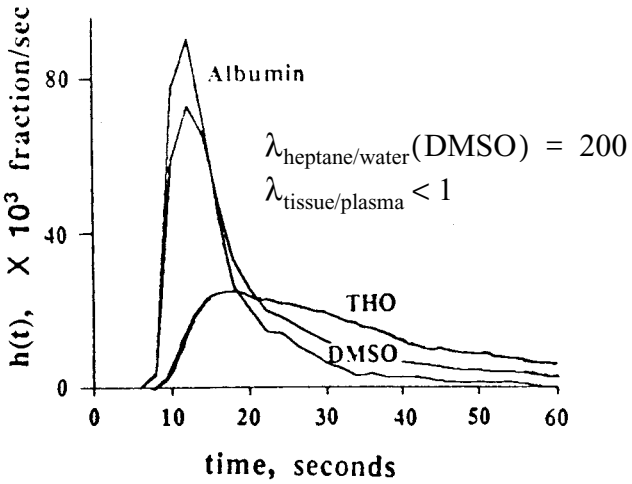

Figure 9-2: Outflow indicator-dilution curves in an isolated, perfused rabbit heart preparation. The volume of distribution for DMSO, which rapidly permeates membranes, is not much larger than is the volume of distribution for the albumin, which is almost completely confined to the vascular space.

9-2.4. Passive equilibration

Passive equilibration is the mechanism that governs the partition coefficient for most solutes. Consider an inert hydrophilic molecule small enough to permeate membranes and with a low solubility in lipids and membranes. The molecule dissolves in the water and its partition coefficient is close to that for water. The partition coefficient for water, or tracer-labeled water, is the water fraction of the "tissue" relative to that for plasma. The water fraction of plasma is about 0.94 ml/ml (Altman and Dittmer, 1971); since the plasma specific gravity, ρ_{pl}, is about 1.035 (Merrill and Wells, 1961), the plasma water is about 0.94/1.035 or 0.91 g/ml, that is, 0.91 ml of water per gram of plasma. The water fraction of erythrocytes is about 0.73 ml/ml (Effros and Chinard, 1969), or with an RBC specific gravity of 1.098 g/ml (MacLeod, 1932), or on a per gram basis, 0.73/1.098 or 0.66 ml/g. Erythrocytes are probably the driest cells in the body. From these data the erythrocyte-to-plasma partition coefficient for water, $\lambda_{RBC/pl}$ (water), is 0.73/0.94 or 0.78.

For solutes which distribute in the water space and are not metabolized or bound, then the expected RBC-to-plasma partition coefficient will be close to that for water. This should be the case for L-glucose and mannitol (which, however, are slow to enter), urea, 3-0-methyl-glucose and other small, neutral hydrophilic solutes.

9-2.5. Molecular exclusion

The molecular exclusion mechanism tends to reduce the availability of solvent water to the hydrophilic solutes. The physical basis for this is diagrammed in Fig. 9-3: a solute dissolved in the tissue water cannot enter water which is rendered inaccessible by a matrix of proteins or structural elements such as cytoskeleton or interstitial collagen. This is steric exclusion.

For albumin, the interstitial exclusion is large, around 50%, but depends greatly on the tissue and local physiological status. The ISF albumin concentration is thus much lower than in either plasma or lymph. When local, prenodal lymph has the same albumin concentration as plasma, then one could safely assume that there was equilibrium between albumin in plasma, interstitium,

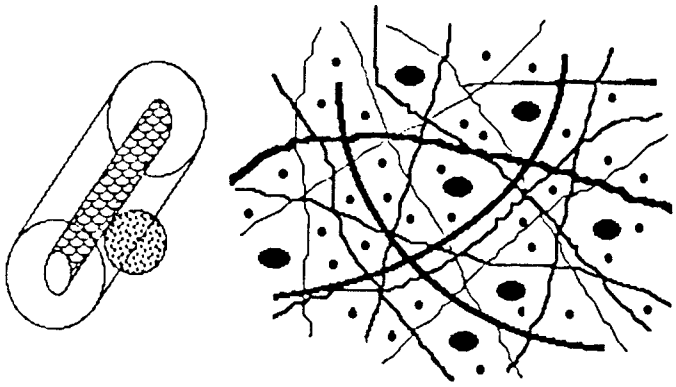

Figure 9-3: Molecular steric exclusion by a meshwork of fibers. *Left panel:* The minimal distance between the fiber axis and a sphere center is the sum of their radii. Water from which a sphere center is excluded is $\pi((r_{cyl} + r_{sph})^2 - r_{cyl}^2)$ per unit length of fiber, so the solute concentration near the fiber is reduced relative to the bulk fluid. *Right panel:* More water is available to a small solute than a large solute.

and lymph. In this situation one would feel secure that molecular exclusion was the explanation for a reduced albumin concentration. (High capillary pressure and high lymph flow also cause a reduction in ISF/plasma concentration ratios for large proteins.) [no parens -ed.]

9-2.6. The effects of charge

The ionic charge of the solute relative to the charges on the macromolecules residing in the particular space also has an effect on exclusion. A negatively charged solute will tend to be excluded from the neighborhood of fixed negative charges. The result is a reduced volume of distribution relative to a neutral solute of the same size. This has been observed in the interstitium. In a comparison of sulfate and sucrose spaces, Macchia et al. (1979) found that these two extracellular marker solutes occupied the same volume of distribution in rat myocardium, but in rat gastrocnemius the sulphate was partially excluded. The conclusion was that the concentrations of negatively charged sites were higher in the gastrocnemius, and were either not present or were balanced by positively charged sites in the heart. They also found an opposite case in the skeletal muscle of a toad in which the sulfate was more concentrated than the sucrose. These kinds of behaviors are diagrammed in Fig. 9-4.

9-2.7. Intraregional binding enlarges the partition coefficient

The partition coefficient is influenced by binding either in plasma space or in the tissues. Strong binding in the plasma reduces tissue/plasma partition coefficients. For some substances, there are specific plasma protein carriers: retinone, testosterone, and other steroids. Fatty acids are approximately 99.94% bound to albumin at 0.4 mM. For a substance which is free in the plasma, remains extracellular, but binds in the interstitium, then the interstitium/plasma partition coefficient is increased by the binding. At equilibrium,

$$\lambda_{ISF/pl} = \frac{C_{ISF}(\text{free}) + C_{ISF}(\text{bound})}{C_{pl}}. \qquad (9\text{-}4)$$

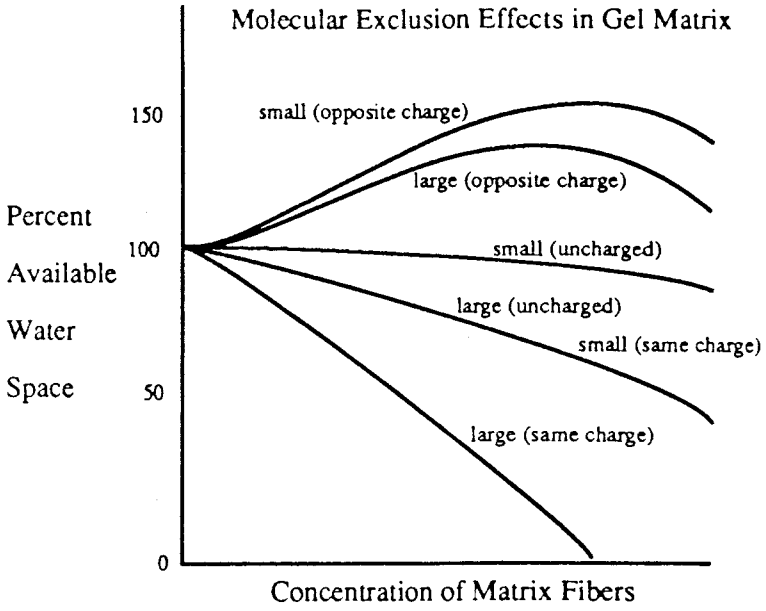

Figure 9-4: Effect of molecular size and charge on apparent volume of distribution for hydrophilic solutes in water containing a matrix of fibers with charged surfaces. Small and large refer to molecular size and parenthetic phrase refers to molecular charge relative to charge on matrix fibers. [source of figure? -ed.]

When the concentration of the binding sites and the dissociation constant are known, then one can translate this expression into one which gives a partition coefficient as a function of the free concentration in the plasma. (Single-site binding expressions are described in Chapter 5 on diffusion and Chapter 8 on transporters.) Under this circumstance the effective interstitial volume of distribution, V'_{ISF}, for this solute is then concentration-dependent, being higher at low concentrations when few of the binding sites are filled and lower at high concentrations when the binding sites are saturated. Such binding must be taken into account with respect to its influence on the diffusion of the free species (Safford and Bassingthwaighte, 1977). The virtual volume of distribution, V', for some solute in a region of volume V is increased by the presence of a substance to which it binds and unbinds rapidly. Consider the binding to a protein of concentration B in the region, for which the dissociation constant for the solute is K_d. Then the equilibrium ratio of the total amount in the region to the amount of free solute is dependent on the solute concentration, C, in the region:

$$\frac{V'}{V} = 1 + \frac{B}{K_d + C} = 1 + \frac{B/K_d}{1 + C/K_d}. \qquad (9\text{-}5)$$

In this expression, the 1 represents the ratio in the absence of binding, and the $B/(K_d + C)$ represents the bound solute in the form of a complex with the protein. C is the concentration of free solute. With $C \ll K_d$, then $V'/V \cong 1 + B/K_d$. With $C \gg K_d$, $V' = V$. The impact of binding is shown in Fig. 9-5 for a protein, B, at two concentrations, 0.5 and 1.0 mM. The protein has a single binding site with a dissociation constant of 0.1 mM. At low solute concentrations the volume of distribution is enlarged by B/K_d, a factor of 11 for $B = 1$ mM.

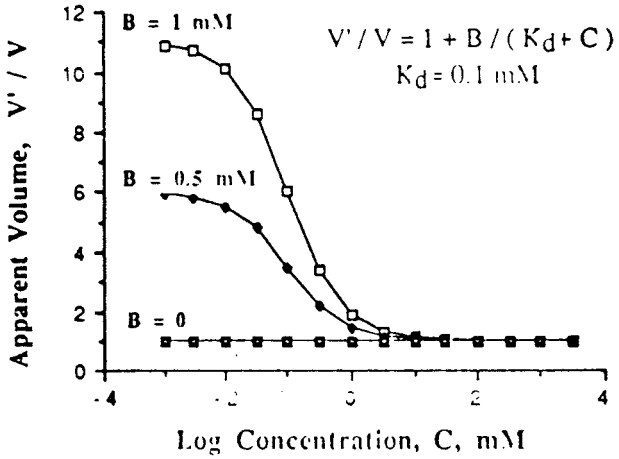

Figure 9-5: In the presence of a binding site of concentration B mM, with a dissociation constant, K_d, of 0.1 mM for the solute, the effective equilibrium volume of distribution is increased, particularly at low concentrations. Curves are for $B = 1$, 0.5, and 0 mM.

The dependence of an apparent λ on physiological state is exemplified by Xe, the "washin and washout" of which is commonly used as a measure of organ blood flow, F_{bl}. The transit time through an organ is

$$\bar{t} = \lambda_{org} V_{org} / F_{bl} = (\lambda_{tiss-bl} V_{tiss} + V_{bl}) / F_{bl} .$$

Here λ_{org} is the organ-to-blood partition coefficient. The second expression gives more detail and distinguishes the blood within the organ from the nonblood tissue (a distinction that Shakespeare's Shylock would approve, no doubt). Because Xe binds to hemoglobin, the relative *amount* of Xe in RBC versus plasma depends on the hematocrit. Because the tissue equilibrates with the RBC by exchanging with plasma, it means that λ is lower at high hematocrit than at low hematocrit (Carlin and Chien, 1977), in accord with Eq. 9-5.

9-2.8. Transmembrane electrochemical potentials influence λ

Another source [Other sources -ed.] of partition coefficients other than one are membrane transport processes that work against gradients in electrochemical potential for specific solutes. Ionic transports are the prime example, including the pumps and the exchangers. For K, the Na/K ATPase accumulates K inside the cell to a level about thirty times that in the surrounding extracellular fluid space. Thus. for cellular potassium, the partition coefficient λ_{K^+} is

$$\lambda_{K^+} = \frac{[K^+]_{cell}}{[K^+]_P} = \frac{150 \text{ mM}}{5 \text{ mM}} = 30 , \text{ so that} \qquad (9\text{-}6)$$

$$V'_{cell}(K^+) = \lambda_{K^+} V_{cell} . \qquad (9\text{-}7)$$

For ions pumped out of cells, the cell/plasma partition coefficient is < 1. For Na, $\lambda_{cell} \cong 0.1$; for Ca^{2+} it is lower yet.

In conditions where the equilibrium concentrations are driven by physiological processes, it is obvious that λ is not a constant, and that while it acts like a solubility ratio, the underlying process is more complex.

9-2.9. pH affects partitioning of acids and bases

Intracellular pH is normally less than extracellular pH, around 7.0 inside versus 7.4 outside. In a hypoxic working muscle the pH can be several-fold lower. How this influences the partition coefficient depends on the pK_a for the acid solute; a diminution in intracellular pH reduces λ for weak acids and raises it for weak bases. A list of the effects pH has on solute partitioning in solution and across membranes is given below [recast list items as sentences -ed.].

1. Affects ratio of dissociation to associated forms of weak acids and bases.
2. Determines fraction of solute available to dissolve in membrane in uncharged form. (Important for substances which are lipophilic when not dissociated.)
3. Determines fraction of solute available for reaction or binding in dissociated form.
4. Dissociated free form distributes in accord with Nernst potential.
5. Undissociated form, permeating membranes more readily, gives access to intracellular organelles.

9-3. Anatomic and virtual volumes

Anatomic observations on capillary densities provide estimates of the blood volume in the exchange region. In well-perfused organs like the heart, liver, kidney, brain and lung the capillary densities are high, as for example in the heart in Fig. 9-6. From the capillary densities and diameters one can estimate volumes of the exchange region. Other estimates need to be put together with these to make sure that the overall properties of volume, specific gravity, tissue composition and water content are all compatible with one another. Such data are shown in Table 9-1.

A more physiological measure of the volume fractions into which specific solutes equilibrate is obtained by determining the volumes of distribution of tracer-labeled solutes of different classes. A comparison of two different extracellular markers in the quick-frozen hearts of rabbits is shown in Fig. 9-7. ^{58}CoEDTA is a particularly good marker because it is a gamma-emitter and the cobalt is extremely tightly bound to the EDTA; the compound is polar and inert and remains extracellular (Bridge et al., 1982). The ^{14}C-sucrose and ^{58}CoEDTA were injected intravenously 25 minutes before sacrificing the animal so that equilibration could occur between blood and extravascular space. The volumes of distribution represent $V'_{ecf} = V_p + V'_{isf}$ where V'_{ecf} ml/g is extracellular fluid space, V_p is the total plasma space, ml of plasma per gram of tissue, and V'_{isf} is the interstitial space, which is the extravascular, extracellular distribution space. The estimates of V'_{ecf} can be used to derive V'_{isf} when V_p is measured by means of an intravascular, plasma marker such as ^{131}I-albumin.

In other experiments Gonzalez and Bassingthwaighte (1990) determined V_p, V_{rbc} (erythrocyte space), V'_{Na} (sodium space) and total water space. For the tracers, the calculation of volume of distribution V'_{tracer}, ml/g, is

$$V'_{tracer} = \frac{1}{\rho_p} \cdot \frac{C_{tracer}\ (\text{heart sample})}{C_{tracer}\ (\text{plasma sample})}, \tag{9-8}$$

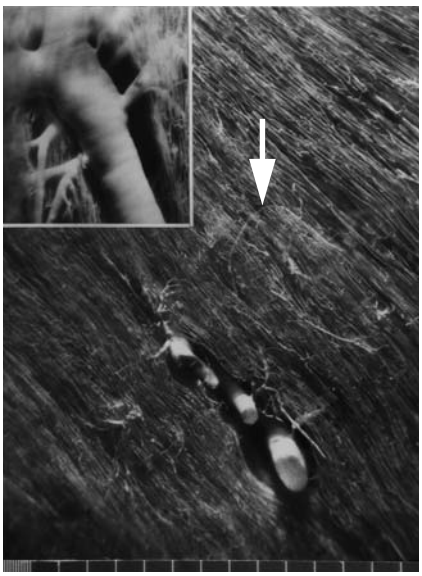

Figure 9-6: Subepicardial vasculature of the dog heart, as shown in section parallel to epicardium, 1 mm deep. Scale divisions are 10 and 100 μm. A 60 μm arteriole, accompanied by two venules, gives rise to three 10 μm arterioles, two short and one long (arrow). Inset (same scale) shows a 160 μm vein giving rise to small venules and branching rapidly into the parallel capillaries. (From Bassingthwaighte et al., 1974, with the permission of Academic Press.)

where C_{tracer} has the units of radioactivity level per gram of tissue or plasma and ρ_p is the specific gravity, g/ml, of plasma. The prime on the V' is therefore a statement that the volume of distribution is a virtual volume with a concentration equal to that in the plasma. The observations for the set of tracers are shown in Fig. 9-8. In this case there is no true extracellular marker like sucrose or CoEDTA, but sodium space V'_{Na} is only slightly larger than V'_{ecf} since the intracellular Na levels are normally less than one-tenth of the extracellular levels.

9-4. Volume and specific gravity of tissue components

Now we are obliged to more specific about what we mean by "tissue." When trying to account for solute, cell, tissue mass, etc., the estimated tissue and plasma partition coefficient is closer to 1 when the tissue contains a lot of plasma. In practice, when one takes small tissue samples, avoiding large vessels, the plasma content is lower than when the whole organ is quick frozen. The sampling technique does not affect any of the partitioning effects, but only influences what we define as tissue. The safest, most consistent estimates of λ will be obtained by excluding the intratissue plasma from the computation. The closer one can get to $\lambda_{ISF/plasma}$ or $\lambda_{cell/pl}$, the better that λ can be understood on a physical and chemical basis.

9-4.1. An experimental procedure for intraorgan volumes of distribution

An example of a general procedure used to obtain estimates of volumes of distributions is that of Gonzalez and Bassingthwaighte (1990), but it should be appreciated that there were many prior studies of a similar nature which yielded information on distribution spaces within organs. In this example we omit the use of microspheres for estimating flow distributions. For the experiment,

Table 9-1: Constituents of the Heart

					Source reference
Total mass as percent of body weight					
Human 0.45					Diem, 1962
Baboon 0.35					King et al., 1985
Regional myocardial mass and blood flows:					
Region	Sp. gr.	Mass Fraction, %	Fraction of Flow, %	Mean Flow, ml min^{-1} g^{-1}	
Left ventricle	1.063	75	80	1.0	Polimeni, 1974
Right ventricle	1.062	20	17	0.8	Bassingthwaighte et al., 1974
Atria		5	3	0.6	
Left ventricle tissue fractions					Polimeni, 1974
Cells	70%				
Interstitium	16%				
Capillaries	3.5%				
Arteries and veins	10%				
Capillary dimensions (arrayed in parallel)					Bassingthwaighte et al., 1974
Functional lengths	500–1,000 μm				
Diameters (mean ± SD)	5.0 ± 1.3 μm (SD)				
Capillary density	3,100–3,800/mm^2				
Intercapillary distance	17.5–19 μm				
Chemical composition:					

	Composition, %		
Component	by weight	by volume	
Water	78	82.6	Yipintsoi et al., 1972
Fat	1.5	1.67	Dible, 1934
Protein	17	12.5	Diem, 1962
Carbohydrate	0.7	0.7	Diem, 1962
Mineral ash	1.1	0.5	Diem, 1962

take tritium-labeled water (THO), ^{58}CoEDTA as an extracellular marker, ^{131}I-labeled albumin as a plasma space marker, and ^{51}Cr-labeled RBCs. At time = 0 inject THO (100 μCi); at t = 120 min. inject ^{51}Cr-labeled RBCs (50 μCi); at t = 150 min. inject ^{131}I-labeled albumin (10 μCi) and ^{58}CoEDTA (20 μCi). At times 120, 160, 170 and 179 minutes, obtain samples of plasma for the measurement of tracer concentrations; obtain the last sample just prior to sacrifice. Sacrifice at

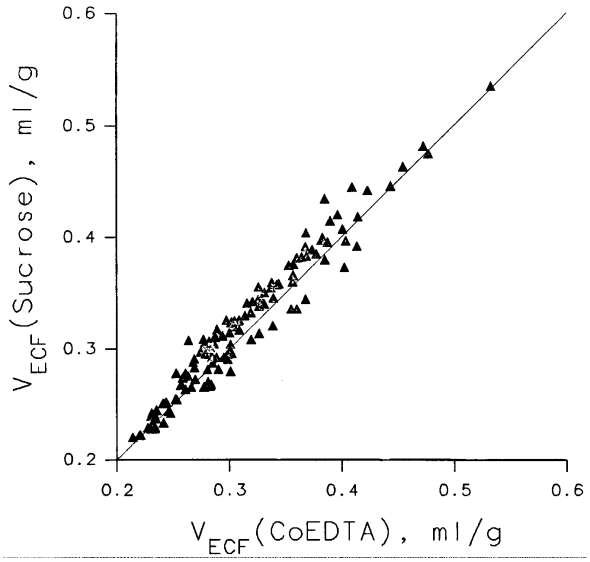

Figure 9-7: Estimates of volumes of distribution of extracellular markers. A comparison of extracellular fluid space (V_{ecf}) estimates from [^{14}C]sucrose versus ^{58}Co-EDTA (from γ-counting rather than β-counting). Regression line, V_{ecf}(Suc) = 0.001 + 1.03 V_{ecf}(^{58}Co-EDTA), with a correlation coefficient of 0.974, is not distinguishable from line of identity. Average V_{ecf} for two tracers is 0.32 ± 0.06 (N = 130) ml of plasma-equivalent volume/gram of myocardium. (Figure from Gonzalez and Bassingthwaighte, 1990.)

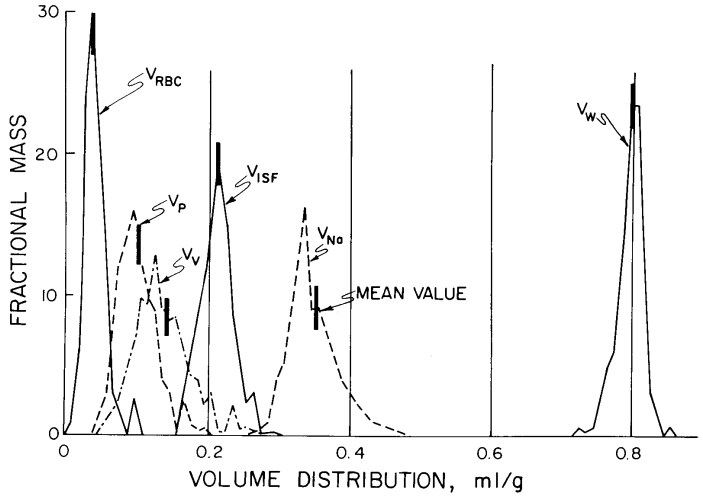

Figure 9-8: Probability density functions of volumes of distributions in rabbit left ventricle. Density functions for six animals are combined by superimposing the mean of each individual heart upon the average mean; this provides a correct and realistic representation of spread of the data around the mean. (Figure from Gonzalez and Bassingthwaighte, 1990.)

180 minutes. Divide the heart into multiple small samples. Measure the concentrations (cpm/g) of the various tracers in each of the pieces.

9-4.2. Definition

The volume of distribution, V_r, for region *r* is milliliters per gram, so that the total tissue volume per gram occupies less than a milliliter when the specific gravity, ρ, is greater than 1.0 g/ml. We shall also use the term V'_r, where the prime indicates that this is the regional plasma equivalent volume expressed as a "virtual," as opposed to "real" volume equivalent to the volume of plasma at equilibrium concentration. The relationship between the virtual and real volume is given by the actual ratio of concentrations at steady state:

$$V'_r = \frac{C_r}{C_{pl}} \cdot V_r , \tag{9-9}$$

where the tracer concentrations are cpm/g.

To account for both mass and volume, the specific gravity of each tissue component is needed. The total tissue volume per gram is

$$V_{tissue} = V_{RBC} + V_{pl} + V_{ISF} + V_{cell} , \tag{9-10}$$

and the mass of 1 gram is

$$\rho_{tissue} V_{tissue} = \rho_{RBC} V_{RBC} + \rho_{pl} V_{pl} + \rho_{ISF} V_{ISF} + \rho_{cell} V_{cell} . \tag{9-11}$$

From these expressions one can see that the tissue specific gravity is a weighted average of that for the individual regions:

$$\rho_{tissue} = \rho_{RBC} \frac{V_{RBC}}{V_{tissue}} + \rho_{pl} \frac{V_{pl}}{V_{tissue}} + \rho_{ISF} \frac{V_{ISF}}{V_{tissue}} + \rho_{cell} \frac{V_{cell}}{V_{tissue}} . \tag{9-12}$$

In a later section we shall relate the specific gravities to the composition of the region, in terms of its fractions of water, fat, and protein and solutes. High protein tissues are more dense than water: for heart muscle, $\rho_{tissue} = 1.063$ (Yipintsoi et al., 1972); The calculations to obtain the volumes of distribution are applied using the observed tracer concentrations in a particular space compared with its concentration in the tissue, for example using A for ^{131}I-albumin (assuming it is strictly intravascular) and measuring its concentration in plasma and in the tissue:

$$V_{pl}, \text{ml/g} = \frac{1}{\rho_{pl}} \cdot \frac{C_A(\text{tissue})}{C_A(\text{plasma})} \quad \text{with} \quad \rho_{pl} \simeq 1.035 \text{ g/ml} , \tag{9-13}$$

where V_{pl} is the volume of plasma per gram of tissue. Likewise for RBC,

$$V_{RBC}, \text{ml/g} = \frac{1}{\rho_{RBC}} \cdot \frac{C_R(\text{tissue})}{C_R(\text{RBC})} \quad \text{with} \quad \rho_{RBC} = 1.098 \text{ g/ml} . \tag{9-14}$$

C_R (RBC) is the value for centrifuged erythrocytes corrected for trapped plasma (trapped plasma is 3% to 4%). These two values define the intratissue hematocrit. The blood hematocrit in large vessels, Hct_{LV}, is

$$Hct_{LV} = \frac{\text{volume of RBC}}{\text{volume of blood}} = \frac{V_{RBC}}{V_{RBC} + V_{pl}}, \tag{9-15}$$

and the intratissue hematocrit is defined the same way:

$$Hct_{tissue} = \frac{V_{RBC}}{V_{RBC} + V_{pl}}. \tag{9-16}$$

This points to the fact that the volume of distribution of blood in the tissue is

$$V_{blood} = V_{RBC} + V_{pl}. \tag{9-17}$$

The blood weight fraction of the tissue is $\rho_{pl}V_{RBC} + \rho_{pl}V_{pl}$, and the blood volume fraction of the tissue is $(V_{RBC} + V_{pl})/V_{tissue}$. Intratissue hematocrit is lower than for large vessels: Gonzalez and Bassingthwaighte (1990) found the average ratio, $Hct_{tissue}/Hct_{LV} \cong 0.77$ in rabbit ventricular myocardium; Phelps et al. (1979) found a value of 0.85 for the **??** brain.

The ECF is more complicated because it is composed of the plasma plus the interstitial fluid (ISF). The basic formula is where C_E is the extracellular marker concentration:

$$V_{ECF} = \frac{1}{\rho_{ECF}} \cdot \frac{C_E(\text{tissue})}{C_E(\text{ECF})}, \tag{9-18}$$

where C_E is the extracellular marker concentration. Neither ρ_{ECF} nor C_E (ECF) can be measured directly. To estimate C_E (ECF) and C_E (ISF), first choose an inert solute that does not bind in the ISF or plasma, is not influenced by charge, and does not enter cells, but is small enough so that molecular exclusion from the extracellular water space is negligible. L-glucose (no glucose transporter affinity), and mannitol are satisfactory. Gonzalez and Bassingthwaighte's (1990) choice of ^{58}CoEDTA was based on a desire to use a gamma-emitting tracer. They showed that ^{58}CoEDTA space is equal to sucrose space in the rabbit myocardium; this shows that neither of these molecules is significantly excluded since ^{58}CoEDTA is larger (MW = 422) than sucrose (MW = 342) and therefore should have entered a smaller space than sucrose if there were molecular exclusion.

The unknowns C_E (ECF) and ρ_{ECF} are both composites of ISF and plasma. When there is evidence of molecular exclusion, then the concentration in the water of the ISF and plasma should be equal:

$$C_E(\text{ISF}) = \lambda_{ISF/pl} \cdot C_E(\text{plasma}), \tag{9-19}$$

with $\lambda_{ISF/pl} = 1.0$ on the basis of equal degrees of exclusion, etc., in plasma and ISF. Assuming also that $\rho_{ISF} = \rho_{pl}$, then

$$V'_{ECF} = \frac{1}{\rho_{pl}} \cdot \frac{C_E(\text{tissue})}{C_E(\text{plasma})}. \tag{9-20}$$

From this one can see, and we now state explicitly, that V_{ECF} is a "plasma-equivalent" volume. So when we derive V'_{ISF},

$$V'_{ISF} = V'_{ECF} - V_{pl}; \tag{9-21}$$

we recognize also that V'_{ISF} is a plasma equivalent volume. The assumptions regarding ρ_{ISF} and C_E(ISF) are not easy to avoid, but they are not too bad for small neutral solutes.

From this we calculate the water space in the ECF:

$$V_{ECF}(\text{water}) = (\text{water fraction of plasma, ml/ml}) \cdot V'_{ECF}. \tag{9-22}$$

The prime indicates that this is a virtual volume of distribution, a plasma-equivalent space, but in this case it should be close to the real anatomical volume of the ECF.

Polimeni (1974) compared estimates of V'_{ISF}. Tracer estimates and electron micrograph morphometry estimates were reassuringly close in the rat heart left ventricular tissue. For tracer estimates, sulphate space was 0.197 ± 0.008, and glucose space was 0.181 ± 0.005; for morphometric estimates of the interstitial space, 0.192 ± 0.005. This might suggest the presence of anionic binding sites in the ISF as an explanation for the larger sulfate space than glucose space or morphometric estimate. Later work by Macchia et al. (1979), however, revealed substantial differences between the two tracers in rat *skeletal* muscle: sulphate space of 0.105 ± 0.006, and glucose space of 0.150 ± 0.007, quite the reverse ratio of what was found in heaart muscle. Naturally large solutes have a smaller V'_{ISF} due to molecular exclusion; for albumin only half the space is available: V'_{ISF} (albumin) ≈ $0.5V'_{ISF}$ (sucrose).

The same approach is used for volumes of distribution in the cells of tissue. There is currently only one method for determining cell volumes for any specific cell type, namely morphometrical estimation from histological preparations (Weibel, 1979, 1980). With tracer techniques all are lumped together simply as water space unavailable to extracellular solutes. For practical purposes in measuring water space one may use any marker which is dominantly hydrophilic, so that it serves as a marker for water space, and yet permeates membranes easily. Our choice is water itself, using DHO or THO if tracers are needed, or simply taking the difference between wet and dry weight.

$$V_w = \frac{1}{\rho_w} \cdot \frac{W(\text{wet}) - W(\text{dry})}{W(\text{wet})}, \tag{9-23}$$

where ρ_w is the specific gravity of water, close to 1.0 g/ml. The tracer method of our example uses

$$V'_w = \frac{1}{\rho_w} \cdot \frac{C_w(\text{tissue})}{C_w(\text{plasma})}. \tag{9-24}$$

Because plasma is only 94% water by volume, the true water space, V_w, is smaller:

$$V_w = (\text{water fraction of plasma, ml/ml}) \cdot V'_w. \tag{9-25}$$

The two methods for estimating V_w, Eqs. 9-23 and 9-25, should give the same result. To our knowledge, no such comparison has been made. Total water spaces in soft tissues are just under 80% (see Table 9-2).

Table 9-2: Fractional volumes FIX THIS!!

Organ and variable	Volume (%)	Reference
Heart:	79–80 (water)	Altman and Dittmer (1971)
plasma	10	Gonzalez and Bassingthwaighte (1990)
RBC	3.8	
ISF	20	
cell	67	
Liver:		
ISF	6.0 (Albumin)	Goresky (1963)
	8.0 (Sucrose)	
RBC	15 ± 6	
cell water	55	
Kidney:	87 (water)	
blood	23 ± 2	Effros et al. (1967)
ISF	18 ± 4	
tubular and cellular	62 ± 9	
Brain:		Patlak and Fenstermacher (1975)
ISF	17.2 ± 0.6	
blood	3.5 ± 1.5	Budinger (1981)

The intracellular water space is estimated by difference:

$$\begin{aligned} V_{cell}(\text{water}) &= V_w - V_{ECF} \\ &= (\text{water fraction of plasma, ml/ml}) \cdot (V'_w - V'_{ECF}) \\ &\simeq 0.95(V'_w - V'_{ECF}) \end{aligned} \quad . \tag{9-26}$$

The estimated V_{cell} (water) is smaller than the true anatomic volume. Most cells are not as dry as erythrocytes, and are closer to 75% water; however, the variation is wide. Fat cells with fully loaded lipid vacuoles may be only 20% water.

Summarizing to this point, the primes on the Vs indicate that they are virtual volumes, that is, plasma-equivalent volumes of distribution and not true anatomical volumes. The unprimed volumes may be regarded as follows: V_{pl} is the actual volume of the plasma, but its water content is approximately 94%. V_{RBC} should be the true red cell volume in one gram of tissue. V'_{ECF}

represents the plasma-equivalent volume of distribution in the extracellular space and equals the true V_{ECF} if the solid contents of the ISF and plasma are the same. In tracer experiments we will usually use the concentration in the plasma as the intra-experiment reference, so that we will usually use the V's, the virtual plasma equivalent volumes.

The dog heart has a specific gravity, ρ_H of 1.063 g/ml (Yipintsoi et al., 1972) and a water content, W_H, of 0.78 ml g^{-1} (Yipintsoi et al., 1972). Since the volume of one gram of myocardium is 1/1.063, the total of heart volume is 0.94 ml g^{-1} and the water fraction is 0.78/0.94 or 83% by volume. These numbers mean that the heart is composed of solids of only 17% by volume or 22% by weight. The wet weight/dry weight ratio is 1/0.22 or 4.5.

These numbers illustrate that the volumes of distribution do not add up to the tissue volume. There is a residual fraction of the volume that is not necessarily inaccessible to solute but is unavailable to dissolve solute. Observed this way, the maximum space available for a hydrophilic solute free in solution is the water space. Lipophilic solutes dissolve in membranes and in lipid vacuoles, as well as in the water space, and therefore have slightly larger volumes of distribution. Even so, their tissue/blood partition coefficients do not often exceed 1.0.

9-4.3. Applying conservation principles to masses and volumes

Now let us seek proper totals accounting for both mass and volume and water content by summing up the regions. The conservation equations for volume, mass, and water content are

$$V_{tissue}, \text{ ml/g tissue} = V_{RBC} + V_{pl} + V_{ISF} + V_{cell} = \frac{1}{\rho_{tissue}}, \tag{9-27}$$

$$\text{mass per gram heart tissue} = \rho_{RBC}V_{RBC} + \rho_{pl}V_{pl} + \rho_{IFS}V_{IFS} + \rho_{cell}V_{cell} = 1.0, \tag{9-28}$$

$$\text{water content, ml/g tissue} = V_{RBC}W'_{RBC} + V_{pl}W'_{pl} + V_{ISF}W'_{ISF} + V_{cell}W'_{cell} = \frac{W'_{tissue}}{\rho_{tissue}}. \tag{9-29}$$

where the units are ρ, g/ml; V, ml/g; and W, ml/ml. Of the terms used in these three expressions, five are not known. These are ρ_{ISF}, ρ_{cell}, V_{cell}, W'_{ISF}, and W'_{cell}. Having five unknowns and only three equations one has to find either good reasons for guessing at two of the unknowns, or alternatively, to generate some new information. Taking the former course of action, one could reduce the number of unknowns by making judicious assumptions. For example, assume that $\rho_{ISF} = \rho_{cell}$, and that $W'_{ISF} = W'_{cell}$, thereby reducing the number of unknowns to three.

The alternative strategy is to add information. Another type of measurement that can be made on a tissue relates to its composition of fat, protein, and nonprotein solutes in addition to water. These components have different specific gravities: fat, 0.901 (Allen et al., 1959); protein, 1.38 (Allen, Welch et al. 1959); and water, 1.0 g/ml. By lumping protein and nonprotein solids together with approximate specific gravity of 1.38 g/ml, one can describe the tissue by a point on a diagram such as Fig. 9-9.

For any region, or for the whole tissue, the following relationships, defined in slightly different notation than used by Yipintsoi et al. (1972), hold for the water content (W' ml/g), the fat content (F' ml/g), and the protein combined with other nonfat solids (P' ml/ml):

$$W' + P' + F' = V_{tissue}, \text{ ml/g}, \tag{9-30}$$

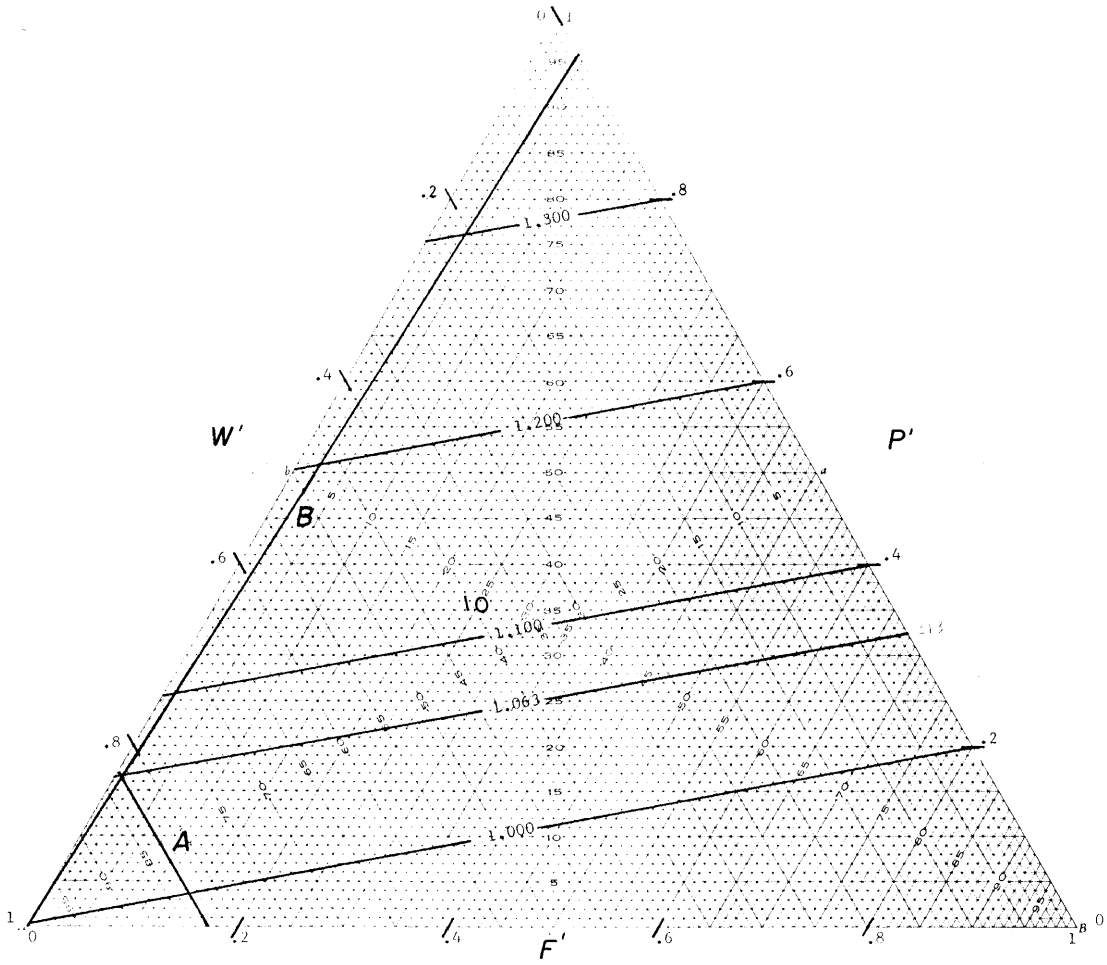

Figure 9-9: Diagram to estimate the density from the myocardial content of water (W'), fat (F'), and protein plus other nonfat solids (P'). For any given ratio of P'/F', the gain or loss of water from the myocardium moves the point defining the tissue along a line between the W' apex and the point on the P'/F' line defining that ratio.

$$\rho_W W' + \rho_P P' + \rho_F F' = \rho_{tissue} V_{tissue} = 1.0 \text{ g/g}. \tag{9-31}$$

These are all directly measurable; for example, F' ml/g, is the fat content in grams per gram tissue divided by ρ_F. The diagram has the limited virtue of showing how the specific gravity changes as a function of composition. To apply the knowledge of composition to help determine the unknowns requires bringing the two points of view together.

Consider the fat. Erythrocytes have none, plasma fat is measurable, interstitial fat is essentially zero, and the remainder of tissue fat is in cells. Expressions similar to Eq. 9-30 and Eq. 9-31 can be stated for each region, and the totals must add up. For example, using unprimed F, P, and W to denote composition in g/g, we have

$$P_{tissue}, \text{ g/g tissue} = \rho_{RBC} V_{RBC} P_{RBC} + \rho_{pl} V_{pl} P_{pl} + \rho_{ISF} V_{ISF} P_{ISF} + \rho_{cell} V_{cell} P_{cell}, \tag{9-32}$$

and similar expressions for F and W. The expression for F is more simple because ISF and RBCs are fatless:

$$F_{\text{tissue}},\ \text{g/g tissue} = \rho_{\text{pl}} V_{\text{pl}} F_{\text{pl}} + \rho_{\text{cell}} V_{\text{cell}} F_{\text{cell}}, \tag{9-33}$$

when F_{tissue} and F_{pl}, V_{pl} and ρ_{pl} are measured, then the amount of cell fat is known, and is the last phrase in Eq. 9-33, but none of the components of the plasma are known. The W_{tissue}, g/g, is known since it is $\rho_{\text{W}} V_{\text{tissue}}$ (water); likewise, $W_{\text{pl}} = \rho_{\text{W}} V_{\text{pl}}$ (water) and $W_{\text{RBC}} = \rho_{W} V_{\text{RBC}}$ (water), but W_{ISF} and W_{cell} are unknown.

At this point we have enlarged the number of unknowns to 9 (ρ_{ISF}, ρ_{cell}, V_{ISF}, V_{cell}, P_{ISF}, P_{cell}, F_{cell}, W_{ISF}, W_{cell}), all because we do not know the true volumes, V_{ISF} and V_{cell}. We assume F_{RBC} and $F_{\text{ISF}} = 0$. We have 17 knowns or measurables. The desired equations aggregate knowns and measurables to equal a measurable; specific gravities, total compositions, mass, and volume provide the ten summarizing equations. The first five are whole tissue expressions and the last four are for the ISF and cell regions:

$$1.0\ \text{g/g} = \rho_{\text{RBC}} V_{\text{RBC}} + \rho_{\text{pl}} V_{\text{pl}} + \rho_{\text{ISF}} V_{\text{ISF}} + \rho_{\text{cell}} V_{\text{cell}}, \tag{9-34}$$

$$V_{\text{tissue}},\ \text{ml/g} = \frac{1}{\rho_{\text{tissue}}} = V_{\text{RBC}} + V_{\text{pl}} + V_{\text{ISF}} + V_{\text{cell}}, \tag{9-35}$$

$$P_{\text{tissue}},\ \text{g/g} = \rho_{\text{RBC}} V_{\text{RBC}} P_{\text{RBC}} + \rho_{\text{pl}} V_{\text{pl}} P_{\text{pl}} + \rho_{\text{ISF}} V_{\text{ISF}} P_{\text{ISF}} + \rho_{\text{cell}} V_{\text{cell}} P_{\text{cell}}, \tag{9-36}$$

$$F_{\text{tissue}},\ \text{g/g} = 0 + \rho_{\text{pl}} V_{\text{pl}} P_{\text{pl}} + 0 + \rho_{\text{cell}} V_{\text{cell}} P_{\text{cell}}, \tag{9-37}$$

$$W_{\text{tissue}},\ \text{g/g} = \rho_{\text{RBC}} V_{\text{RBC}} W_{\text{RBC}} + \rho_{\text{pl}} V_{\text{pl}} W_{\text{pl}} + \rho_{\text{ISF}} V_{\text{ISF}} W_{\text{ISF}} + \rho_{\text{cell}} V_{\text{cell}} W_{\text{cell}}, \tag{9-38}$$

$$\text{cell: } 1.0,\ \text{g/g} = P_{\text{cell}} + F_{\text{cell}} + W_{\text{cell}}, \tag{9-39}$$

$$\text{ISF: } 1.0,\ \text{g/g} = P_{\text{ISF}} + 0 + W_{\text{ISF}}, \tag{9-40}$$

$$\text{cell: } \frac{1}{\rho_{\text{cell}}},\ \text{ml/g} = \frac{P_{\text{cell}}}{\rho_{\text{P}}} + \frac{F_{\text{cell}}}{\rho_{\text{F}}} + \frac{W_{\text{cell}}}{\rho_{\text{W}}}, \tag{9-41}$$

$$\text{ISF: } \frac{1}{\rho_{\text{ISF}}},\ \text{ml/g} = \frac{P_{\text{ISF}}}{\rho_{\text{P}}} + 0 + \frac{W_{\text{ISF}}}{\rho_{\text{W}}}. \tag{9-42}$$

The solution can now be calculated using a nonlinear optimizer since we have nine equations for nine unknowns. This slight degree of "overdeterminedness" is beneficial; there is enough error in the measurables to render the solution rather inexact. An example of a result is given in Table 9-3.

Table 9-3: Data from studies of myocardium (1 = Yipintsoi et al., 1972; 2 = Gonzalez and Bassingthwaighte, 1990; 3 = Merrill and Wells, Jr., 1961; 4 = Altman and Dittmer, 1971 based on $\rho_P = 1.4$, $\rho_F = 0.9$, $\rho_W = 1.0$ g/ml; 5 = MacLeod, 1932; 6 = Effros and Chinard, 1969; 7 = Dible, 1934; 8 = White et al., 1978).

Variable: name, units	Measured value (reference)	Estimated value (confidence range)
ρ_{tissue}, g/ml	1.063 (1)	
ρ_{pl}, g/ml	1.035 (3)	
ρ_{RBC}, g/ml	1.098 (4,5)	
ρ_{ISF}, g/ml		1.005 (± 0.01)
ρ_{cell}, g/ml		1.087 (± 0.008)
$V_{tissue} = 1/\rho_{tissue}$, ml/g	0.941 (1)	
V_{pl}, ml/g	0.07 (2)	
V_{RBC}, ml/g	0.041 (2)	
V_{ISF}, ml/g		0.26 (± 0.03)
V_{cell}, ml/g		0.57 (± 0.03)
W_{tissue}, g/g	0.78 (1)	
W_{pl}, g/g	0.95 (4)	
W_{RBC}, g/g	0.66 (6)	
W_{ISF}, g/g		0.9 (± 0.04**??**)
W_{cell}, g/g		0.7 (± 0.04**??**)
P_{tissue}, g/g	0.91 ( )	
P_{pl}, g/g	0.08 (8)	
P_{RBC}, g/g	0.504 ( )	
P_{ISF}, g/g		0.1 (± 0.04)
P_{cell}, g/g		0.26 (± 0.01)
F_{tissue}, g/g	0.02 (7)	
F_{pl}, g/g	0.005 (8)	
F_{RBC}, g/g	0 ( )	assumed = 0
F_{ISF}, g/g		assumed = 0
F_{cell}, g/g		0.03 (± 0.01)

9-4.4. From composition back to partition coefficients

Solute partitioning is not defined by the processes that govern solute distribution and the simplistic expressions of regional composition. However, these ideas lead to an understanding of how to estimate a partition coefficient when cellular metabolism prevents tracer from reaching an equilibrium state. After all, our greatest interests are in solutes that react or stimulate reactions, that is, substrates or hormones.

The glucose partition coefficient and volumes of distribution are estimated by analogy. Instead of glucose, the intracellular concentration of which is lowered by metabolism, we use 3-O-methyl-glucose. It is transported across cell membranes by the glucose transporter, and equilibrates across the membranes with equal concentrations on the inside and outside because it undergoes no metabolic reactions, nor does it bind to sites inside or outside the cell. 3-O-methyl-glucose is insoluble in lipid so its volumes of distribution are virtually the same as for water. A general expression for a partition coefficient in terms of regional volumes of distribution is

$$\lambda_{\text{tissue}/\text{pl}}\,(\text{solute}) \;=\; \sum_{\text{r}} \rho_{\text{r}} V_{\text{r}} \lambda_{\text{r}/\text{pl}}\,. \tag{9-43}$$

For glucose, we escape the problem of trying to discover the $\lambda_{r/pl}$ by assuming that 3-O-methyl-glucose spaces and water spaces coincide:

$$\lambda_{\text{r}/\text{pl}} \;=\; \frac{\Sigma_{\text{r}} \rho_{\text{r}} V_{\text{r}} W_{\text{r}}}{\rho_{\text{pl}} V_{\text{pl}} W_{\text{pl}}} \;=\; \frac{\rho_{\text{tissue}} V_{\text{tissue}} W_{\text{tissue}}}{\rho_{\text{pl}} V_{\text{pl}} W_{\text{pl}}}\,, \tag{9-44}$$

(all these values can be found in Table 9-3.) The calculation gives $\lambda_{r/pl}$ (3-O-methyl-glucose) = 10.

9-4.4.1. The oxygen partition coefficient

This is more complex because of binding by hemoglobin in the RBCs and by myoglobin in the myocardial cells. There is no myoglobin in endothelial cells. We split the process into two parts: find $\lambda_{RBC/pl}$ and the partition coefficient for the extravascular, nonflowing region separately. Because oxygen's solubility in lipids is low, if there were no binding or consumption it would presumably distribute in uniform concentration in the water space.

For the RBCs, oxygen dissolves in its water and also binds to hemoglobin in a concentration-dependent fashion:

$$\lambda_{\text{RBC}/\text{pl}} \;=\; \frac{C_{\text{RBC}}\,(\text{free}) + C_{\text{RBC}}\,(\text{bound})}{C_{\text{pl}}}\,. \tag{9-45}$$

This can be done experimentally because the RBCs consume no oxygen; erythrocytes derive energy via glycolysis to form lactate. The details of how to calculate this from the oxygen tension and the hemoglobin concentration are covered in standard texts and used in models for oxygen exchange (Groebe, 1990). Oxygen dissolved in plasma or RBC water is 0.0029 ml O_2 per 100 ml solution per mmHg P_{O_2}; at an oxygen partial pressure of 100 mmHg, 1 ml of plasma carries 0.0029 ml O_2. In blood, the hemoglobin concentration is about 0.15 g/ml, and at 100 mmHg P_{O_2}, it binds 0.21 ml O_2. In addition the RBC water carries dissolved oxygen, which is almost negligible in comparison, about 0.002 ml O_2 per ml RBCs (0.0029 times 0.65, the water fraction of the RBC volume). From this, for oxygen at a P_{O_2} of 100 mmHg,

$$\lambda_{\text{RBC}/\text{pl}} \;=\; \frac{C_{\text{RBC}}(\text{free}) + C_{\text{RBC}}(\text{bound})}{C_{\text{pl}}(\text{free})} \;=\; \frac{0.002 + 0.21}{0.0029} \;=\; 73\,. \tag{9-46}$$

At a P_{O_2} of 26 mmHg, hemoglobin carries half as much oxygen, so $\lambda_{RBC/pl} = (0.0005 + 0.105)/0.0007 = 150$, twice as high as at 100 mmHg simply because of the high affinity of hemoglobin for O_2. Hemoglobin affinity for CO is 210 times greaterthan for oxygen, so that 0.1% CO in the air blocks 75% of hemoglobin's capacity for O_2 transport.

In myocardial cells, myoglobin concentration is about 0.5 mM or 0.015 g/ml, one tenth that of hemoglobin. Its dissociation curve is for single site binding with a K_d between 2.5 and 5 mmHg P_{O_2}. So at 100 mmHg P_{O_2}, myoglobin is saturated carrying 0.5 mM O_2 or 0.0112 ml O_2/ml in bound form in the cytosol. Adding bound and unbound at $P_{O_2} = 100$ mmHg,

$$\lambda_{cell/pl} = \frac{0.0024 + 0.0112}{0.0029} = 4.7 .$$

Now a tissue/blood partition coefficient can be calculated. First, consider only the extravascular tissue versus the blood and use $\lambda_{ISF/pl} = 1.0$:

$$\lambda_{extravascular/blood} = \frac{(\lambda_{ISF/pl} \cdot V_{ISF} + \lambda_{cell/pl} \cdot V_{cell})/(V_{ISF} + V_{cell})}{(\lambda_{RBC/pl} \cdot V_{RBC} + V_{pl})/(V_{RBC} + V_{pl})} \simeq 0.135 . \qquad (9\text{-}47)$$

This means that even in the absence of oxygen consumption and with myoglobin saturated, most of the oxygen is in the blood. The actual ratio of blood oxygen to tissue oxygen with zero consumption is

$$\frac{O_2 \text{ in extravascular regions}}{O_2 \text{ in blood}} = \frac{V_{ISF} + \lambda_{cell/pl} \cdot V_{cell}}{V_{pl} + \lambda_{RBC/pl} \cdot V_{RBC}} = \frac{0.2 + 4.7 \times 0.6}{0.06 + 73 \times 0.04} = \frac{3.02}{2.98} \approx 1.0 . \qquad (9\text{-}48)$$

Thus, with blood occupying only 10% of the tissue, it carries as much oxygen as tissue containing myoglobin, and even a larger fraction when tissue consumption is high..

With consumption, tissue P_{O_2} is lowered to an average of about 3 mmHg, just about the 50% saturation point for myoglobin. ($\lambda_{cell/pl} \approx ((0.0024 \times 0.03) + 0.0056)/0.001 \approx 5.7$). Likewise, the P_{O_2} decreases in blood between inflow and outflow, outflow P_{O_2} being close to 26 mmHg. Using Eq. 9-48 with the altered λs,

$$\lambda_{extravascular/blood}(O_2, \text{ tissue consuming}) = 0.07 ,$$

which is about half of the value in the absence of consumption. So there is a two times higher fraction of O_2 in the blood when the tissue is consuming than when it is not. All of these values are approximate, and the equations can be used to obtain more suitable values for specific situations.

9-5. Kinetics of dilution and distribution

The estimation of volumes of dilution or volumes of distribution, while based on a simple conservation of mass, is complicated by the fact that the dilution of material introduced into a region does not necessarily occur very quickly. An example is the use of the kitchen blender: with it half filled with water and turned up to full speed add some dye to the middle of the vortex (or anywhere else) and observe how quickly the equilibration occurs. By eye it may look like 10 to 15

seconds, but if one uses a continuous sampling through a densitometer to measure the dye concentration, it will be found that at thirty seconds mixing is still incomplete. This observation by itself should make one suspicious that the proverbial mixing chambers are, generally speaking, figments of the mathematical simplifications that one uses to make problems manageable. If events are slower than expected, it may happen that enough time elapses so that even relatively slow events can complicate the simple principles.

Complicated behavior costs analysis time and introduces sources of error. This has been understood for a long time. Sjostrand, in his review in the *Handbook of Physiology* (1962), reported that mannitol was used as a marker for extracellular water space, on the basis that it was not soluble in lipids and therefore did not cross cell membranes; the truth is that if mannitol were to mix rapidly in the water of the extracellular fluid, e.g., within a few circulation times around the body, then the concentration measured would give a rather good estimate of extracellular space. However, what really happens is that the recirculation and distribution to regions of the body with high blood flows like the heart, kidneys, and brain goes through many recirculations while the mixing in slow flow regions of limbs, cold skin, and cerebral spinal fluid takes at least ten to thirty minutes or more. Mannitol does enter cells, though slowly during this time, and its loss from the extracellular fluid space, ECF, lowers its concentration in the plasma and causes an overestimate of the ECF volume. Given a longer time, mannitol becomes a marker for body water space: since it is not consumed in mammalian tissues it simply equilibrates, and in the 1930's it was used as a measure of total body water space, until it was replaced by the use of deuterated water, D_2O (Edelman, 1952), which equilibrates much more quickly. D_2O has the additional advantage that it's fractional loss over the two to three hours required for equilibration is less than for mannitol (excreted via glomerular clearance) since the total water loss by perspiration, pulmonary loss and urinary loss is rather small, a few hundred milliliters out of 70% of body mass.

9-6. Dilution in a well-stirred volume

The expression for the quantity of a solute in a fluid volume is

$$q_0 = CV\,, \tag{9-49}$$

where q_0 is the amount of material in moles, C is the concentration of the equilibrated fluid in that volume, moles/liter, and V is the volume in liters.

It is implicit in this expression that C is the same everywhere within the volume; we assume that this is a uniformly mixed volume of distribution for the substance whose concentration is being measured. This works quite well in a well-stirred beaker (Fig. 9-10). If we wish to know how great the volume in the beaker is, we can take a known amount of solute, q_0, inject it into the beaker, mix well, sample the concentration to obtain a measure of C and thereby estimate V from this equation:

$$V = q_0/C\,. \tag{9-50}$$

This expression is the basis for huge numbers of studies of human and animal physiology, and studies in general throughout the world of science. Equation 9-49 is a statement of conservation of mass: the left side of the expression, q_0, is the mass injected into the fluid; the equation states that the concentration times the volume is the mass, q_0. Equation 9-49 also shows

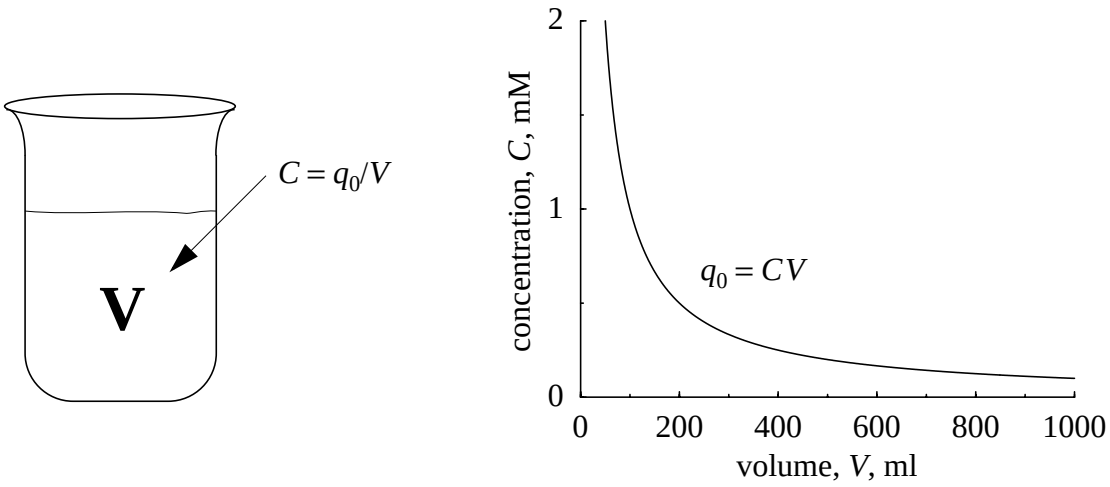

Figure 9-10: Dilution of mass q_0 in volume V results in concentration C. The relationship between C and V is a hyperbola.

the hyperbolic relationship: when q_0 is put into a small volume the concentration is high; when q_0 is put into a large volume, the concentration is low.

In applying the volume of distribution principle, Eqs. 9-49 and 9-50 are based on the assumption that an equilibrium has been reached; mixing throughout the volume, by convection and by diffusion or dispersion throughout, have reached a balance wherein molecular movement produces no more changes in concentration throughout the volume. Molecular diffusion, Brownian motion, and thermal collisions are the quantum mechanical events; concentration in a solution is a continuum idea, a summary, at a more global level of description. In physicochemical terms one can say that this solution, at the given temperature and pressure, is at its state of maximum entropy or lowest potential energy, and that all potential gradients have been dissipated. Having reached this happy state via molecular dispersion or mechanical stirring, the fancy physicochemical statements mean only that the system has degraded to its lowest energy state, and that the further lapse of time does not lead to a further lowering in energy. Without energy input, water flows downhill until it comes to the bottom and stays there.

Passive processes, convective or diffusive, dissipate potential energy gradients. In sizable, well-stirred systems, mixing occurs mainly by convection, and diffusion plays an important but secondary role. Consider a system designed so that there is no stirring, only diffusion. An example is a familiar science classroom display: a water-filled graduated cylinder with copper sulfate crystals at the bottom, and the top sealed to prevent evaporation. Even with mixing caused by trucks rumbling by and stampeding herds of students coming and going, the blue color remains deeper at the bottom of the column than at the top for months or even years. In such a column the higher specific gravity of the saturated copper sulphate solution at the bottom inhibits the convective mixing caused by the rumbling truck. There is no driving force to cause the fluid at the bottom of the cylinder to rise by convection toward the top. Diffusion dominates, but it is slow. This is quite different from solutions where viscous fingering occurs (Comper and Laurent, 1978), in which convective and diffusive interactions produce vertical columns that protrude from the lower layer of fluid into the upper layer.

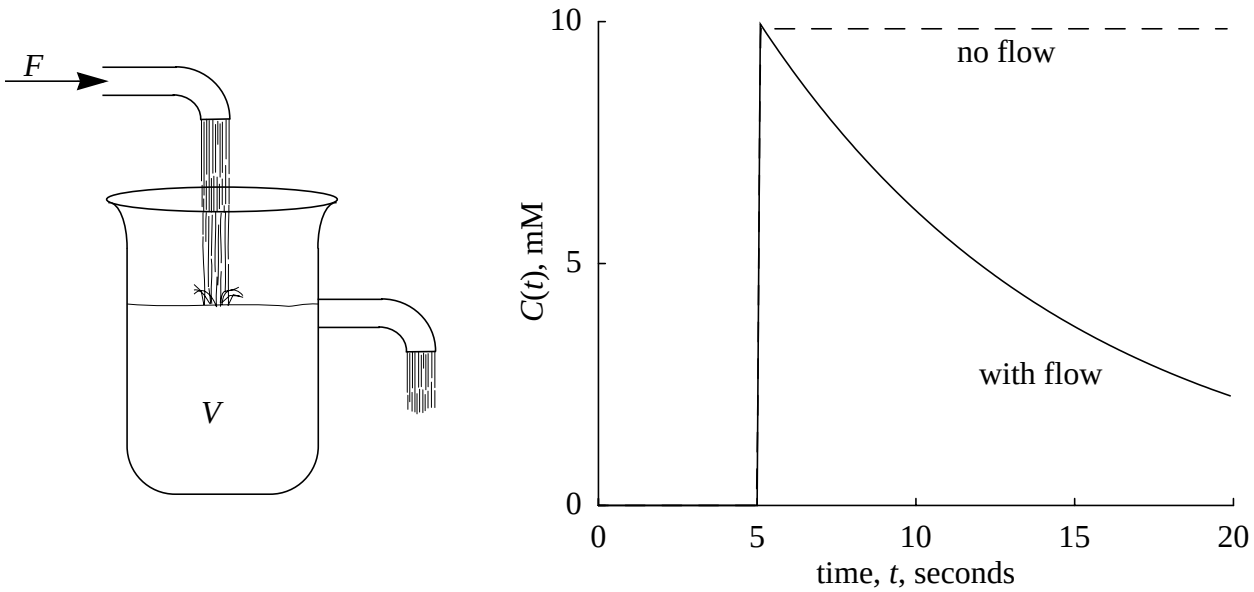

Figure 9-11: Displacement of fluid from a well-stirred chamber. (Values are $F = 10$ ml s^{-1}; $V = 100$ ml; $q_0 = 1$ mmole injected at $t_0 = 5$ s. The concentration-time curve is $C(t) = (q_0/V) \cdot e^{-Ft/V}$.)

9-6.1. Fluid displacement from a well-stirred tank or perfect mixing chamber

When there is a flow, F, into the mixing chamber diagrammed in Fig. 9-11, then the same principles apply as for fluid displacement through a pipe. With an impulse input of solute mass, q_0, into the entrance to the chambers, the content, $q(t = 0_+)$, is initially q_0, and the concentration everywhere is instantaneously q_0/V, given instantaneous complete mixing, including the fluid next to the outflow. This is quite different from the pipe model. The rate of washout into the outflow is a fraction of the volume per unit time; the fraction is the volume displaced in that time, F, divided by the chamber volume, V; thus F/V is the fractional escape rate, a constant. Because of the instantaneous mixing, the residual mass of indicator within the chamber, $q(t)$, and the concentration, $C(t)$, have the same shape, but different units.

The concentration-time curve of Fig. 9-11 can be used to estimate the initial volume of distribution even if one cannot sample the initial concentration at $t = 0$ or if the mixing is not instantaneous. The method is to extrapolate the curve of $C(t)$ back to time zero; this can be done for this particular system by plotting log $C(t)$ versus t, then projecting back to obtain an estimate of $C(t = 0)$, and calculate $V = q_0/C(t = 0)$. This is only correct for a purely monoexponential washout.

There is another way to estimate the volume. The mean time for fluid displacement in the beaker can be calculated using the principle that volume is conserved: the volume, V, is displaced by an inflow, F, over a time, $\bar{t}$, i.e., $F\bar{t} = V$. This gives the formula for mean transit time,

$$\bar{t} = V/F, \tag{9-51}$$

just as for the dispersionless pipe. Thus $\bar{t}$ is a "characteristic" time for flow through a mixing chamber; it is the first moment of $C(t)$. If flow is known then $V = F\bar{t}$. This is general and not restricted to the classical "first-order mixing chamber" or "compartment" shown in the figure.

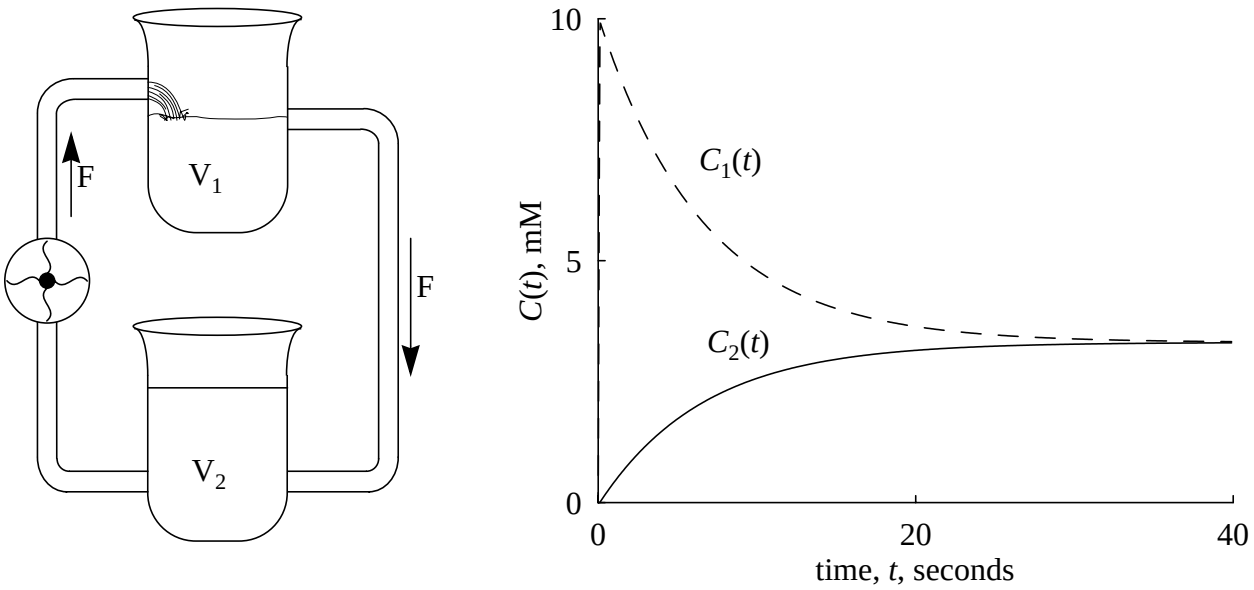

Figure 9-12: Dilution into a pair of well-stirred volumes. *Left panel:* Diagram of an experimental system. The flow is determined by the pump. *Right panel:* Time course of concentrations with pulse input when each of V_1 and V_2 are instantaneously mixed. ($F = 10$ ml s^{-1}, $V_1 = 100$ ml, $V_2 = 200$ ml, $q_0 = 1$ mmole injected at $t = 0$. $C(t = 100\text{ s}) = 3.33$ mM.)

9-6.2. Impeded mixing

Instantaneous mixing is impossible and very fast mixing takes huge energy; therefore, in practical situations, one puts a modest amount of energy into convective mixing and much hope into the idea that diffusion will do the rest.

The left panel of Fig. 9-12 shows a simple situation where some time is required to reach a steady state. There is exchange between the well-stirred volumes V_1 and V_2 via tubing of negligible volume. With V_1 on an upper shelf and V_2 on a shelf below, a pump drives fluid from V_2 up into V_1. The overflow from V_1 flows back to V_2. At time $t = 0_+$, the instant after injection when there is instantaneous mixing in V_1, the concentration, $C_1 = q_0/V_1$. With continuous flow this concentration will be diluted by inflow from V_2, and a part of q_0 is lost into the outflow. The loss from V_1 at the rate governed by the flow provides material to V_2. (The actual flux from V_1 to V_2 is the product of flow times outflow concentration, $F \cdot C_1$ moles/second. In this very special example of a well-stirred chamber, C_1 is the concentration throughout the volume, V_1. There is obviously a second flux of the solute from V_2 to V_1; this is $F \cdot C_2$. Later on we will solve the equations for such fluxes.) After a long time, the concentrations C_1 and C_2 approach a common value, C_∞. When all of the mixing is complete, the concentration provides a measure of the total volume:

$$V_{\text{total}} = V_1 + V_2 = q_0 / C_\infty . \tag{9-52}$$

In practice, this would be the concentration obtained at some reasonably long time, t_2, rather than t_∞. Combining this information with that obtained at t_0, and by sampling V_1 we can calculate V_2:

$$V_2 = V_{\text{total}} - V_1 = \frac{q_0}{C_1(t_2)} - \frac{q_0}{C_1(t = 0_+)} = q_0\left(\frac{1}{C(t_2 \approx \infty)} - \frac{1}{C(t = 0_+)}\right). \qquad (9\text{-}53)$$

Experimentally one might wish to confirm that the concentration, C_2, is equal to C_1 at time t_2. However, there are situations in which V_2 cannot be sampled, for example if V_1 represents plasma and V_2 represents the interstitial fluid. Its volume may be inferred from observations made in V_1 only, as in this example.

One can imagine what might happen to an extracellular marker injected into the plasma. If mixing throughout the circulating plasma space was rapid, and permeation into the extravascular/extracellular fluid space was rather slow, then it would seem possible to make measurements at two instances, as shown in Fig. 9-12, allowing time before the first sampling for mixing to occur in V_1, and then waiting until mixing is thorough and complete between V_1 and V_2 before taking the second sample at time t_2, when equilibrium should have occurred. The practical problem with this approach is that before solutions are completely mixed, there is significant escape from the plasma space by the small solute markers used for estimating extracellular space (Sjostrand, 1962; Lawson, 1962); the mixing times for plasma proteins and red cells are very long. This means that even the measurement of volumes of distribution of the body becomes a little more complicated than just simply injecting a solute and then measuring its concentration after some time.

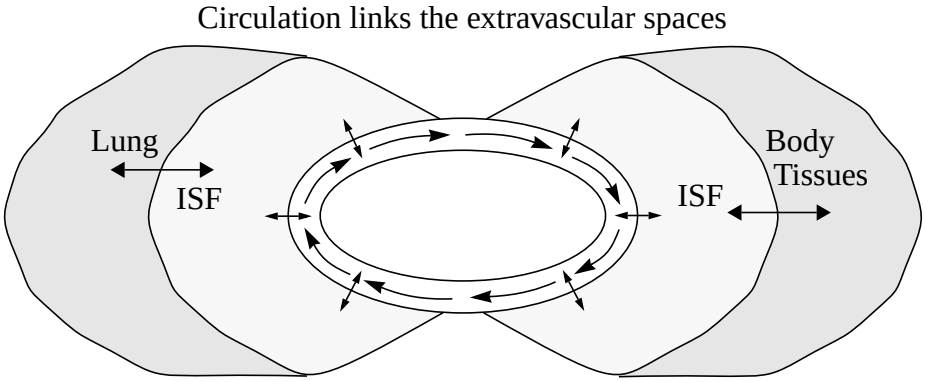

Figure 9-13: A two-region "body." At two extremes this model is the same as that in Fig. 9-12. One extreme is in infinitely rapid exchange between ISF and blood in both "lung" and "body tissues." The other is infinitely rapid flow within a blood space of negligible volume.

9-7. Two regions with flow mixing

The system in Fig. 9-13 is a modified version of that in Fig. 9-12 (left panel). At two different extremes of conditions its behavior looks like that of the system in Fig. 9-12. At intermediate values for flow and exchange rates, the model is different from that of Fig. 9-12. Consider the two extremes first. In one, let there be rapid exchanges between blood and ISF in both the lung and tissues of the body. If the exchange across the barrier between the blood and the ISF space is extremely rapid and the diffusion throughout the ISF space and blood within an organ is extremely rapid, then the "lung" and "tissues of the body" each behave as uniformly mixed chambers and the system is the same as that in Fig. 9-12.

Now consider a very different problem. If the flow is extremely rapid through both lung and body tissues so that the blood has a virtually uniform concentration at all times, then this system would be considered a three-region system with the middle region representing the blood space. When the blood volume is small compared with the ISF volume, then, just as we elected to have negligible volumes for the tubing in Fig. 9-12, V_1 would represent the lung ECF and V_2 the body ECF. Now because the exchange between the two ISF volumes is limited by the rate of exchange between the extravascular spaces and the blood space, we will get a situation that looks kinetically like that of Fig. 9-12 (right panel). If we make an injection into the lung ISF, for example, the concentration will approach the equilibrium value as in Fig. 9-12, but the meaning and explanation will be quite different. There will actually be a concentration in a blood region and it will be intermediate between the concentrations in the two ISF spaces. Furthermore, instead of only the F in Fig. 9-12 representing the conductance between the two volumes, the conductance will be that of the flow and of two membranes, that of the lung ISF to the blood and that of the body tissue's ISF to the blood.

Figure 9-14 gives a more precise illustration. In the system diagrammed in Fig. 9-14, the waveforms for the plasma marker and for the ECF marker have different time courses. The

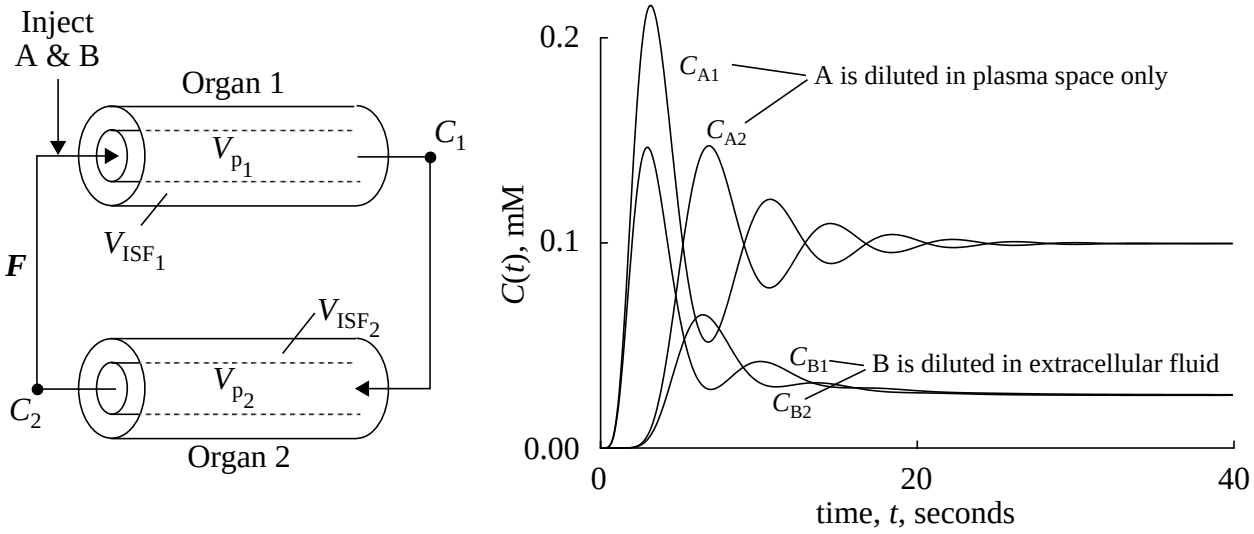

Figure 9-14: *Left panel:* Two-organ, "whole-body" model, each organ composed of a blood plasma region with volume V_p and an extravascular, interstitial fluid region, *ISF*, with volume V_{ISF}. *Right panel:* The response of the system to a pulse injection into the entrance to organ 1, with the concentrations measured at the outflows of this two-organ "whole-body" model. $F = 1$ ml sec^{-1}, $V_{P_1} = V_{P_2} = 10$ ml; $V_{ISF_1} = V_{ISF_2} = 30$ ml; for tracers A and B, $q_0 = 2.0$ μmoles.

concentrations at the outflow of each organ are shown for each of the tracers. If one considers the body as a two-organ system, the pulmonary system and the body, then the outflows from organ 1 represent aortic concentrations and the outflows from organ 2 represent the pulmonary artery concentrations.

In our idealized experiment, the same amounts of solute A, the plasma marker with concentration C_A, and solute B, the marker distributing in both plasma *and* ISF with concentration C_B, were injected simultaneously at the entrance to V_{P1}; consequently, the ECF

marker is diluted to a considerably lower value. In the right panel of Fig. 9-14, after injection into the inflow of organ 1, the concentration-time curves for solutes A and B at each outflow are shown. The outflow curve for A at outflow 1, C_{A1} has a higher peak than that for B because some B has escaped into the ISF. The concentration-time for A is dampened by passage through organ 1 and organ 2, but still has a high enough peak that three more oscillations in C_A are visible. Solute B's oscillations are severely dampened relative to A because the escape into the ISF regions of both organs is only transient, and the tracer returns by reflux (often called "back diffusion") from the ISF to the blood. This reflux would give a long tail of tracer washout that would be evident if there were no recirculation.

From the equilibrium values, one can calculate the plasma space for the total system via C_A, and the extracellular space for the total system via C_B. From such a plot it is evident that there is no steady-state value that gives a measure of the volume of the plasma in organ 1 or in organ 2, and only the sum of the volumes can be calculated without some more-sophisticated analysis. The same statement applies to the extracellular fluid regions: only their sum is available. However, these are informative:

$$V_P = V_{P1} + V_{P2} = q_A / C_{A_\infty}, \tag{9-54a}$$

$$V_{ECF} = V_{P1} + V_{P2} + V_{ISF1} + V_{ISF2} = q_B / C_{B_\infty}, \tag{9-54b}$$

$$V_{ISF} = V_{ECF} - V_P, \tag{9-54c}$$

where V_P, V_{ECF}, and V_{ISF} are the whole-body values. The interstitial fluid space, V_{ISF}, is always calculated by difference. There is no marker that can be isolated to the interstitial space since it always equilibrates with plasma.

For plasma labels, one chooses large proteins which do not escape quickly from the vascular space. To provide good measures of the plasma space it is also important that they not stick to endothelial surface receptors or escape into the extravascular interstitial space of organs with fenestrated endothelial barriers, e.g., the spleen and liver. Traditional plasma markers are listed in Table 9-4 along with some estimates. ^{131}I-labeled human serum albumin has the virtues of fairly good retention of the iodine on the albumin and a reasonably short physical half-life (8.03 days). Moreover, the biological half-life or retention of ^{131}I in the body is quite short when its uptake into the thyroid is blocked. ^{99m}Tc-albumin binds less well but has an even shorter half-life (6 hours) and no uptake into the thyroid. ^{59}Fe-labeled transferrin (mw 76,000–81,000) is a good stable label with an appropriate isotopic half-life (44 days). For studies with Positron Emission Tomography (PET), ^{68}Ga-albumin (half-life 68 minutes) is preferred.

The common red cell markers are ^{59}Fe and ^{51}Cr. ^{51}Cr is a low-energy beta emitter with a 28 day half-life. For PET studies, inhaled ^{11}CO is the choice, for it binds nearly irreversibly to hemoglobin. The time required for mixing and recirculating red cells is longer than that for plasma markers (Sjostrand, 1962; Lawson, 1962). In humans the first main phase of mixing takes 10 to 15 minutes; however, the equilibration of the tracer-labeled red cells with red cells retained within the spleen and bone marrow is considerably longer, so what one usually measures are the circulating red cells. One can attempt to distinguish between the circulating and the noncirculating or stored red cells, just as might be suggested by the diagrams in Figs. 9-13 and

Table 9-4: Whole animal data. (Human data for a 65 kg male, 170 cm tall, 15% body fat.)

Space	Marker	Volume (ml/kg)	Species	Reference
RBC	^{51}Cr-RBC	28	Human	Fairbanks and Tauxe (1967)
Plasma	^{131}I-HSA	45	Human	Sjostrand (1962)
		46	Dog	
ECF Space	^{14}C-sucrose	192	Human	Woodbury (1974)
		213	Dog	
	^{14}C-mannitol	183	Human	
		226	Dog	
	Inulin	170	Human	
		165	Dog	
Body Water Spaces	D_2HO THO Wet/Dry	623	Human	Novak (1967)

9-14, where there is some barrier between the circulating blood and the noncirculating, stored RBC's.

Markers for the extracellular space are a specialized group of hydrophilic solutes. ^{14}C-sucrose and ^{14}C-L-glucose are commonly used since there are no transporters for these sugars to allow them to cross the cell membranes. The glucose transporter of mammalian cells is stereospecific, but bacteria can take up L-glucose and metabolize it. ^{58}CoEDTA is probably the best γ-labeled ECF marker (Bridge et al., 1982) because it is an extremely stable complex, unlike ^{51}CrEDTA, which dissociates slowly. In Table 9-4, ^{14}C-mannitol is listed, but we need to beware since it has also been used to measure body water space; can the timing be so precise that one measures extracellular space at one time and water space at another with the same molecule?

Water space has been measured with deuterated or tritiated water, D_2O or THO, or simply by measuring the weight of the organ before and after drying. Of all the particular spaces, the water space is the least variable from sample to sample in a healthy organ. In the heart, water content is 0.78 ± 0.01 ml/g (Yipintsoi, Scanlon, and Bassingthwaighte, 1972).

Some other solutes partition into tissue with this solubility in water dominating other factors; antipyrine, urea and mannitol are examples; the latter two equilibrate slowly because of membrane barriers. Renal clearance is normally high for mannitol and therefore the expression $V = q_0/C$ cannot be used, except by using back extrapolation to $t = 0$.

The model diagrammed in Fig. 9-14, with solutions shown in the right panel, is composed of two capillary/tissue exchange regions linked with no delay. The capillary/tissue exchange regions could have used the equations of Sangren and Sheppard (1953), and Bassingthwaighte (1974). The numerical representation in our Fig. 9-14, however, was not the sliding fluid element algorithm (Bassingthwaighte, Wang, and Chan, 1989); instead the vascular space was represented by a large series of stirred tanks, each connecting independently with the local extracellular fluid

space. This is the so-called CTEX model (for compartmental blood/tissue exchange), which is analogous to the BTEX models (Bassingthwaighte, Chan, and Wang, 1992) except that there is more dispersion in the vascular space.When the number of stirred tanks is large, the model converges to become identical with the BTEX models. When the number of segments in a CTEX model is reduced to one, this becomes a traditional compartmental model. For a reasonable physiological and numerical representation, the number of segments should be twenty or more. With N = 20, the relative dispersion of the vascular component is $1/\sqrt{20}$, or a relative dispersion of 22%, which is only a little bit higher than that found for dispersion in a large artery (Bassingthwaighte, 1966). For Fig. 9-14 (right panel), $F = 1$ ml g^{-1} min^{-1}, $V_P = 0.1$ ml g^{-1} for both "organs" and the $V_{ECF} = 0.3$ ml g^{-1} for both. The exchange between the plasma space and the extravascular or interstitial space is governed by the capillary permeability-surface area product, *PS*. For the solutions shown, both components used $PS = 1$ ml g^{-1} min^{-1}.

In order to account for tracer dilution in the body water space, the two-region elements were replaced with three-region elements, where one tracer had access only to the plasma space, another to the plasma and ISF spaces, and the third had access to all three regions. For the results shown in Fig. 9-15, the parameter values for the water space tracer were somewhat like those for mannitol, that is, it could enter the extracellular space fairly readily, but was impeded upon entry into the cell space. Parameter values for the plasma and ECF markers were the same as for Fig. 9-14 (right panel); the additional parameter values for the water tracer were that the permeability surface-area product for the cell membrane was 1.0 ml g^{-1} min^{-1}, and the volume distribution was 0.6 ml g^{-1} min^{-1}. It can be seen that the dilution curve for the water tracer is close to that for the extracellular marker during the early part of the solution, but then deviates gradually from it. There was no loss by consumption or excretion for any of these markers.

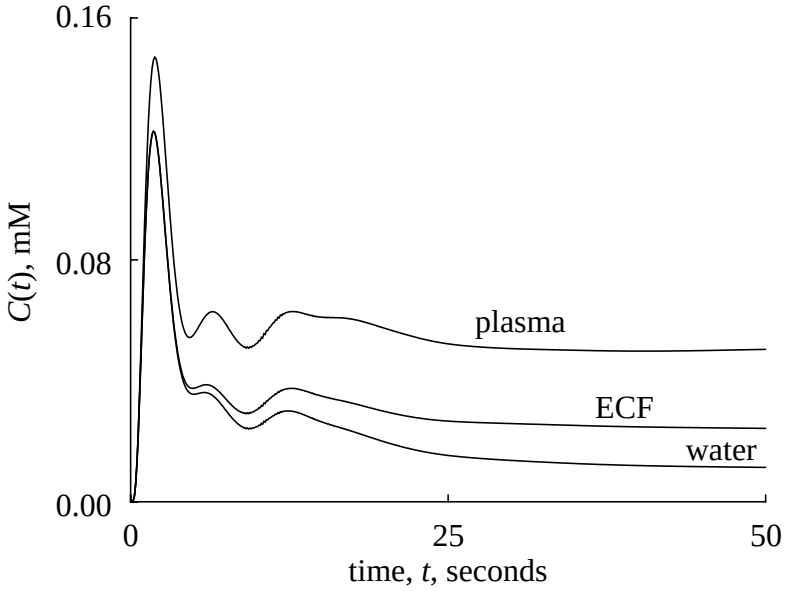

Figure 9-15: Tracer concentration-time courses for a four-organ, three-tissue-region model analogous to that in Fig. 9-14. There was no tracer loss, i.e., zero clearance. Each "organ" was composed of regions for plasma, ISF, and cells. An ECF marker enters the former two regions only; tracer water enters all three regions.

9-8. Plasma space estimation when tracer is lost

The measurement of plasma space using ^{99m}Tc-albumin or indocyanine green (ICG) is not as easy or accurate as it was with Evan's blue dye (T1824) or radioiodinated serum albumin (RISA). The difficulty stems from a continual clearance of the tracer from the plasma space, beginning with the first pass around the circulation before mixing has occurred. A typical shape of curve is shown in Fig. 9-16. This is a model solution, with entirely known parameters for flow exchange and loss, but the shape of the curves are very much like those of Edelman (1952). The traditional approach to estimating a plasma volume is to replot semilogarithmically as in Fig. 9-17, and then to make monoexponential extrapolation back to time 0 to obtain an estimate, $\hat{C}_\infty$, of C_∞, the concentration that would be obtained if there were instantaneous mixing and no clearance. In the exemplary Fig. 9-17, we would estimate $V_P = q_0/\hat{C}_\infty = 0.343$ liters of plasma. But the correct answer was 0.32 liters of plasma. Why is the estimate too high?

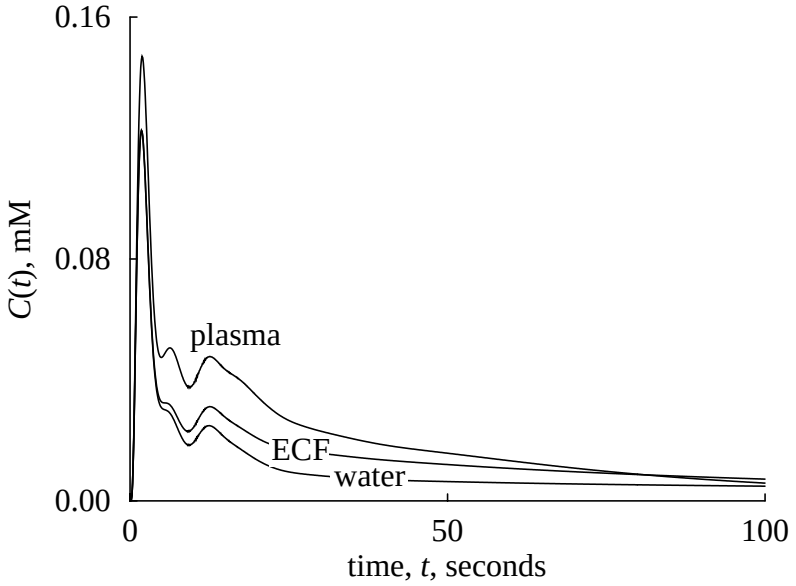

Figure 9-16: Plasma concentration time curves for plasma, ECF, and water markers where there is tracer lost from the body and the clearance is 10% of the flow.

Five model solutions are shown in Fig. 9-18; one for no clearance from the circulation at all, and four for fractional clearances of 5% to 20% of the cardiac output. The monoexponential curves fitted to the "observations" of the last 100 seconds are shown; the lines extrapolate back through the ordinate and have a common intersection at about −7 seconds. The conclusion is that the greater the degree of clearance from the plasma, the smaller the intercept at $t = 0$ and the greater the overestimate of the volume. The slow mixing in the circulation retards the delivery of plasma to the site of clearance; slow mixing has the same effect as a membrane barrier in retarding washout.

There is an earlier time on each curve when the fitted exponentials intersect the horizontal line at the C_∞ that would be obtained with instantaneous mixing. Choosing an extrapolation back "not" to zero, but rather to this earlier time gives a better estimate of the appropriate concentration at equilibrium mixing. Although this is only a specific example and there is no general theory

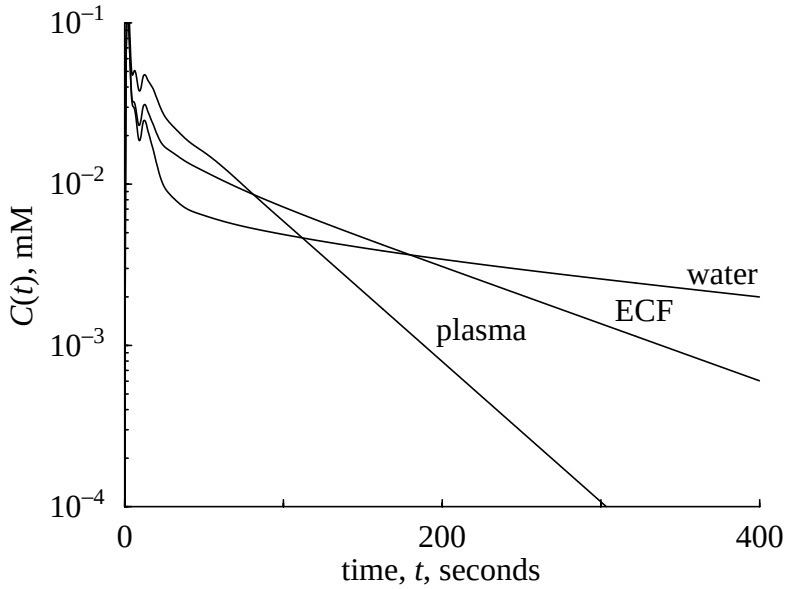

Figure 9-17: Semilog plots of plasma concentrations of markers for plasma, ECF, and water spaces when clearance is exactly 10% of the flow or "cardiac output" in the model diagrammed in Fig. 9-14. All curves eventually have a monoexponential tail. The rate constants are less than 0.10 F/V_r, where V_r is the total volume of distribution of the marker.

worked out, in practice extrapolation back to $t = -7$ seconds does not give error-free estimates, but does change a systematic underestimation of volume into a nearly correct estimate.

An indication of the degree of underestimation of C_∞ and consequent overestimation of V by $V = q_0/\hat{C}_\infty$ is shown in Fig. 9-19. High clearance gives greater overestimation of V. The system represented here is for a rabbit-sized animal with high cardiac output and rather fast mixing. In circulations with greater heterogeneities of transit times through the body, the errors may be larger. The effect of nonmixing is that it retards the clearance relative to that for a mixing chamber.

9-9. Summary

Beware of simple statements about volumes of distribution. The complexities include (1) poor exchange of "tracer with tracee," and long durations required to reach equilibrium; (2) impossibility of reaching equilibrium if tracer is lost; (3) inadequacies of analytical corrections to estimate volumes when the mixing process is complex; (4) partition coefficients being affected by asymmetric transport processes, by the composition of tissues, and by changes in physiological states, so volumes of distribution may change.

The emphasis is on mass conservation. When no tracer is lost, waiting for equilibrium leads to the right answer by $V = q_0/C_\infty$. The common problem for extracellular markers is that there is slow dilution by entry into cells, as well as by renal clearance.

Tissue/plasma and RBC/plasma partition coefficients are measured experimentally. They vary from organ to organ and species to species because of variability in the tissues, particularly

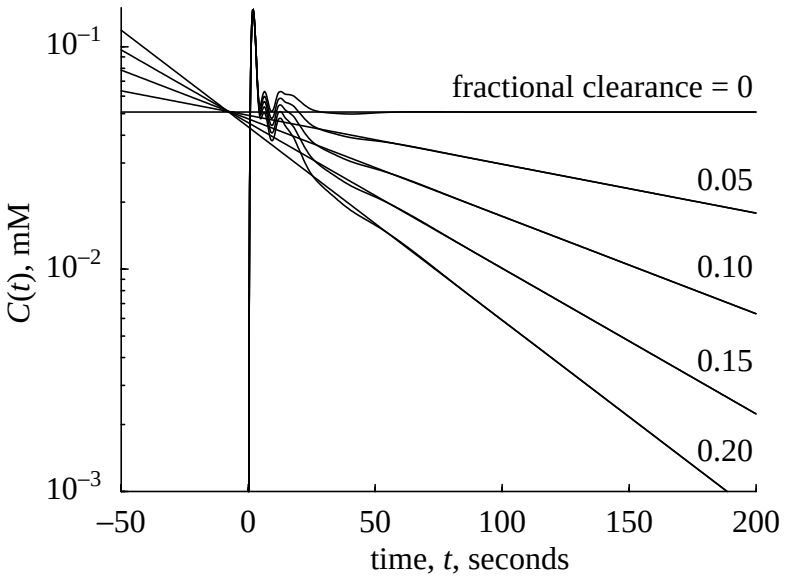

Figure 9-18: Semilog plot of plasma concentration time curves for a strictly intravascular marker which is gradually cleared from the circulation. The tails of the curves are fitted by a single exponential. The loss rate or clearance was set at 0, 5, 10, 15, and 20% of the whole body recirculation. Monoexponential curves fitting the "data" from 100 to 200 seconds extrapolate back to an apparent common intersection at negative time. The intercept at $t = 0$ is lower with clearance > 0, and using its value, $C(t = 0)$, gives overestimates of V_{pl}.

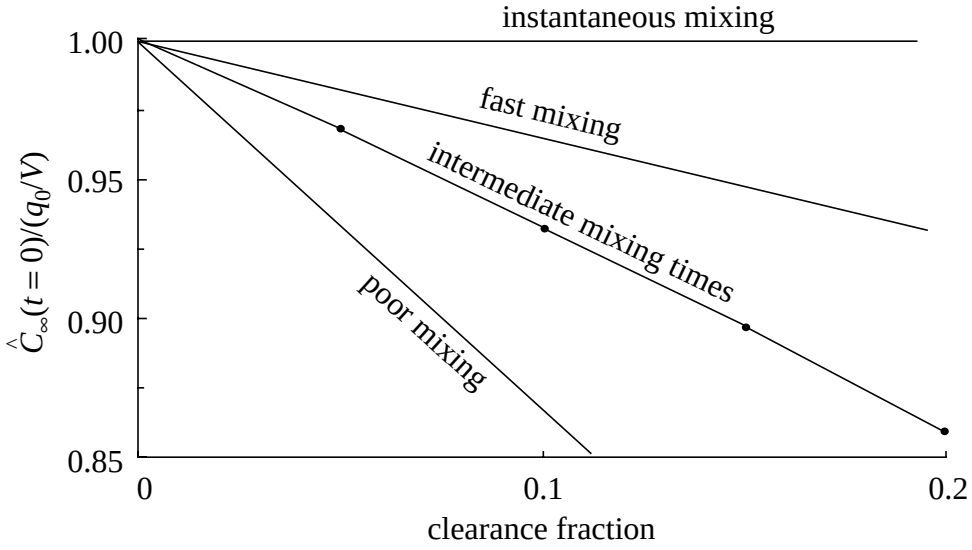

Figure 9-19: Underestimation of equilibrium concentration, $\hat{C}_\infty$, by monoexponential extrapolation to $t = 0$. The line labelled "intermediate mixing times" is that for the "data" of Fig. 9-18. From these intercepts the volume of distributions are *over*estimated by $\hat{V} = q_0/\hat{C}_\infty$. Very rapid mixing gives less error. Heterogeneity of circulation times gives poor mixing.

with respect to chemical composition, and differences in transport mechanisms, and in physical and chemical interactions in different tissue regions.

The strategy we used to figure out the minutiae of interstitial and cellular composition, and specific gravity, provides an example of how conservation of mass, volume, and [conservation of? -ed.] each of the components (water, fat, and protein) can be used to determine regional composition. From the composition, one gains some perception of the various mechanisms by which the equilibration of a solute might occur. The partition coefficients so derived are modified by the more complex processes involved in molecular exclusion, charge, binding, and asymmetrical transmembrane transport.

9-10. Problems

1. In an intact animal an intravenous injection containing ^{131}I-albumin, ^{14}C-sucrose and ^{35}S-sulfate was made at $t = 0$. Tissue samples were taken by biopsy needle. Leg skeletal muscle had a plasma volume of distribution, V'_{pl}, of 0.08 ml/g as determined from the ratio of tracer albumin concentration in a set of muscle samples to a set of plasma samples taken at the same times. For ^{14}C-sucrose the tissue/plasma ratio was 0.28, but for ^{35}S-sulfate the ratio was 0.4. From this information use your best judgement to estimate the volume of the interstitial space in the muscle. How do you interpret the observations for sucrose and sulfate relative to each other. Is your estimate of V'_{isf} compatible with expectations. What about V'_{pl}?

9-11. Further reading

The *Handbook of Physiology* chapters by Sjostrand (1962) and Lawson (1962) are good overviews. Edelman's 1952 review paper is an excellent example of the development that occurred from the 1920's until his time. As a field, body space measurements probably reached their peak in popularity with the publication of *Compartments, Pools, and Spaces in Medical Physiology* (1967), which includes the papers of Novak, and Fairbanks and Tauxe.

Other sources for overviews are handbooks of body composition, and compendia such as the *Merck Index*, and biological handbooks published by FASEB, particularly the handbook authored by Altman and Dittmer (1971).

9-12. References

Allen TH, Welch BE, Trujillo TT, and Roberts JE. Fat, water and tissue solids of whole body less its bone mineral. *J Appl Physiol* 14: 1009-1012, 1959.

Allen TH, Krzywicki HJ, and Roberts JE. Density, fat, water and solids in freshly isolated tissues. *J Appl Physiol* 14: 1005-1008, 1959.

Altman PL and Dittmer DS (Editors). *Respiration and Circulation* Bethesda, Maryland: Federation of American Societies for Experimental Biology, 1971, 930 pp.

Bassingthwaighte JB. Plasma indicator dispersion in arteries of the human leg. *Circ Res* 19: 332-346, 1966.

Bassingthwaighte JB, Yipintsoi T, and Harvey RB. Microvasculature of the dog left ventricular myocardium. *Microvasc Res* 7: 229-249, 1974.

Bassingthwaighte JB. The measurement of blood flows and volumes by indicator dilution. *Medical Engineering* , edited by Ray CD. Chicago: Yearbook Publishers, 1974, p. 246-260.

Bassingthwaighte JB, Wang CY, and Chan IS. Blood-tissue exchange via transport and transformation by endothelial cells. *Circ Res* 65: 997-1020, 1989.

Bassingthwaighte JB, Chan IS, and Wang CY. Computationally efficient algorithms for capillary convection-permeation-diffusion models for blood-tissue exchange. *Ann Biomed Eng* 20: 687-725, 1992.

Bridge JHB, Bersohn MM, Gonzalez F, and Bassingthwaighte JB. Synthesis and use of radiocobaltic EDTA as an extracellular marker in rabbit heart. *Am J Physiol Heart Circ Physiol* 242: H671-H676, 1982.

Budinger TF. Nuclear magnetic resonance (NMR) *in vivo* studies: known thresholds for health effects. *J Comput Assist Tomogr* 5: 800-811, 1981.

Carlin R and Chien S. Partition of xenon and iodoantipyrine among erythrocytes, plasma, and myocardium. *Circ Res* 40: 497-504, 1977.

Comper WD and Laurent TC. Physiological function of connective tissue polysaccharides. *Physiol Rev* 58: 255-315, 1978.

Dible JH. Is fatty degeneration of the heart muscle a phanerosis?. *J Pathol Bacteriol* 39: 197-207, 1934.

Diem K. *Documenta Geigy. Scientific Tables* Ardsley, N. Y.: Geigy Pharmaceuticals, 1962.

Edelman IS. Exchange of water between blood and tissues: characteristics of deuterium oxide equilibration in body water. *Am J Physiol* 171: 279-296, 1952.

Effros RM, Lowenstein J, Baldwin DS, and Chinard FP. Vascular and extravascular volumes of the kidney of man. *Circ Res* 20: 162-173, 1967.

Effros RM and Chinard FP. The *in vivo* pH of the extravascular space of the lung. *J Clin Invest* 48: 1983-1996, 1969.

Fairbanks VF and Tauxe WN. Plasma and erythrocyte volumes in obesity, polycythemia, and related conditions. *Compartments, Pools, and Spaces in Medical Physiology* , edited by Bergner PE and Lushbaugh CC. Oak Ridge, Tennessee: U.S. Atomic Energy Commission, Technical Information Division, 1967, p. 283-298.

Gonzalez F and Bassingthwaighte JB. Heterogeneities in regional volumes of distribution and flows in the rabbit heart. *Am J Physiol Heart Circ Physiol* 258: H1012-H1024, 1990.

Goresky CA. A linear method for determining liver sinusoidal and extravascular volumes. *Am J Physiol* 204: 626-640, 1963.

Groebe K. A versatile model of steady state O_2 supply to tissue. Application to skeletal muscle. *Biophys J* 57: 485-498, 1990.

King RB, Bassingthwaighte JB, Hales JRS, and Rowell LB. Stability of heterogeneity of myocardial blood flow in normal awake baboons. *Circ Res* 57: 285-295, 1985.

Lawson HC. The volume of blood—a critical examination of methods for its measurement. *The Handbook of Physiology: Section 2, Circulation, Volume I* , edited by Hamilton WF and Dow P. Baltimore: Waverly Press, 1962, p. 23-49.

Macchia DD, Page E, and Polimeni PI. Interstitial anion distribution in striated muscle determined with [^{35}S]sulfate and [^{3}H]sucrose. *Am J Physiol* 237: C125-C130, 1979.

MacLeod J. Red-cell density in certain common animals. *Q J Exp Physiol* 22: 275-280, 1932.

Merrill EW and Wells RE Jr. Flow properties of biological fluids. *Appl Mech Rev* 14: 663-673, 1961.

Novak LP. Total body water in man. *Compartments, Pools, and Spaces in Medical Physiology* , edited by Bergner PE and Lushbaugh CC. Oak Ridge, Tennessee: U.S. Atomic Energy Commission, Technical Information Division, 1967, p. 197-216.

Patlak CS and Fenstermacher JD. Measurement of dog blood-brain transfer constants by ventriculocisternal perfusion. *Am J Physiol* 229: 877-884, 1975.
Phelps ME, Huang SC, Hoffman EJ, Selin C, Sokoloff L, and Kuhl DE. Tomographic measurement of local cerebral glucose metabolic rate in humans with (F-18)2-fluoro-2-deoxy-D-glucose: validation of method. *Ann Neurol* 6: 371-388, 1979.
Polimeni PI. Extracellular space and ionic distribution in rat ventricle. *Am J Physiol* 227: 676-683, 1974.
Safford RE and Bassingthwaighte JB. Calcium diffusion in transient and steady states in muscle. *Biophys J* 20: 113-136, 1977.
Sangren WC and Sheppard CW. A mathematical derivation of the exchange of a labeled substance between a liquid flowing in a vessel and an external compartment. *Bull Math Biophys* 15: 387-394, 1953.
Sjostrand T. Blood volume. *The Handbook of Physiology: Section 2, Circulation, Volume I* , edited by Hamilton WF and Dow P. Baltimore: Waverly Press, 1962, p. 51-62.
Stein WD. *Transport and Diffusion across Cell Membranes* Orlando, Florida: Academic Press Inc., 1986.
White A, Handler P, Smith EL, Hill RL, and Lehman IR. *Principles of Biochemistry* New York: McGraw-Hill, Inc., 1978.
Woodbury DM. Physiology of body fluids. *Physiology and Biophysics II: Circulation, Respiration and Fluid Balance* , edited by Ruch TC and Patton RD. Philadelphia: W. B. Saunders Co., 1974, p. 450-479.
Yipintsoi T, Scanlon PD, and Bassingthwaighte JB. Density and water content of dog ventricular myocardium. *Proc Soc Exp Biol Med* 141: 1032-1035, 1972.

TO DO:
1. Redo figure 5 on volumes of distrib with a binding site.
2. More problems.